OPTIMIZATION OF SOLAR TILT ANGLES AND COST EFFICIENCY ACROSS INDIA'S CLIMATIC ZONES

A thesis submitted in partial fulfillment of the requirements for the award of the degree of

BACHELOR OF TECHNOLOGY

In

MECHANICAL ENGINEERING

By

Abhishek Kumar Roy	**21119006**
Aditiya Dudhe	**21119008**
Arikathota Karthik	**21119023**

Under the esteemed guidance of

Dr. Anil Kr. Tiwari

(Professor, NIT Raipur)

DEPARTMENT OF MECHANICAL ENGINEERING

NATIONAL INSTITUTE OF TECHNOLOGY, RAIPUR

November 2024

DECLARATION

We declare that the Project work contained in this report is original and it has been done by us under the guidance of our supervisor. The work has not been submitted to any other University/Institute for the award of any degree or diploma.

Date: 29/11/2024

Signature of the students

Name: Abhishek Kumar Roy
Roll No: 2119006

Name: Aditiya Dudhe
Roll No: 21119008

Name: Arikathota Karthik
Roll No: 21119023

CERTIFICATE

This is to certify that the Project Work entitled “Analysis of possible harvesting of solar radiation in different climatic zone of India using ASHRAE model ” that is being submitted by:

1. Abhishek Kumar Roy 21119006
2. Aditiya Dudhe 21119008
3. Arikathota Karthik 21119023

In partial fulfillment for the award of Bachelor of Technology in Mechanical Engineering to the NIT-Raipur,Chattisgarh, is a record of bonafide work carried out by them under our guidance and supervision.

The results embodied in this thesis have not been submitted to any other University or Institute for the award of any degree or diploma.

Signature of Head of the Department	Signature of the Supervisor
Dr. S L Sinha	Dr. A K Tiwari
Professor	Professor
(Department of Mechanical Engineering)	(Department of Mechanical Engineering)

ACKNOWLEDGEMENT

We would like to express our utmost gratitude towards Dr. Anil Kr. Tiwari , Professor, Mechanical Engineering without whom, we wouldn’t have been able to complete this project. His constant support, innovative ideas, and vision materialized fruitfully into the project. With sincere indebtedness, we thank him for his encouragement and guidance.

We would also like to heartily thank Dr. S L Sinha, Professor, HOD, Mechanical Engineering, for giving us this opportunity of working on this project and providing all the resources necessary from time to time.

Lastly, we would like to thank our respected professors from the Mechanical Engineering department, to whom we will remain forever indebted for providing us with all the knowledge necessary for this project. We would like to extend our gratitude towards our beloved classmates and Alumni who have also helped to create a friendly and helpful environment around us while working on this project.

Abhishek Kumar Roy - 21119006
Aditiya Dudhe - 21119008
Arikathota Karthik - 21119023

Table of Contents

List of Tables

List of Figures

ABSTRACT

The increasing global demand for renewable energy sources has necessitated the optimization of solar energy systems to maximize efficiency and minimize costs. This study focuses on the solar energy potential for urban High-Income Group (HIG) residences across six Indian cities—Raipur, Guwahati, Bengaluru, Amritsar, Bikaner, and Srinagar. Through an analysis of Average Tilt Angle (ATA) and Optimal Tilt Angle (OTA), we identify the variation in solar irradiation, electricity generation, and associated costs on a monthly and seasonal basis.

Key findings reveal that adopting optimal tilt angles can significantly improve electricity generation by up to 12.19%, with yearly cost reductions ranging from ₹22,074 to ₹75,187 per house. Additionally, an analysis of roof area utilization demonstrates that, only 20% of HIG roof areas are required for solar installations, leaving a substantial portion available for other purposes.

The economic and environmental impacts of transitioning from coal to solar power were also evaluated. Solar installations achieved a reduction in electricity production costs of up to 50% and decreased CO_2 emissions by over 94.4%, showcasing substantial potential for environmental sustainability. Annual cumulative savings per house ranged between ₹22,074 and ₹75,187, with government savings exceeding ₹6 crores in Raipur alone that too only from HIG houses.

This research underscores the viability and benefits of solar energy optimization for urban residences, providing a roadmap for sustainable energy practices and informed policymaking.

CHAPTER – I

INTRODUCTION

1.1 INTRODUCTION

Understanding solar energy has become a cornerstone for shaping a sustainable future. Renewable energy sources, particularly solar energy, are critical in advancing sustainability goals. With increasing studies on solar energy, numerous solar appliances have gained prominence. The conversion of solar energy primarily relies on the radiation absorbed by surfaces, whether inclined or horizontal. Beyond powering solar devices, solar radiation also plays a vital role in analyzing building designs and their orientations.

Calculating solar radiation is fundamental for converting solar energy into other forms. In solar appliance analyses, the total irradiation value is crucial as it directly determines the net heat absorbed by a surface. This, in turn, helps accurately assess efficiencies and dimensions. Over time, various theories and empirical relations proposed by researchers have resulted in complex models that often provide site-specific outcomes. One such widely used approach is the ASHRAE model. This model employs empirical equations based on three constants—A, B, and C—to calculate direct, diffuse, and reflected radiation.

1.2 Solar Radiation in Terrestrial Regions

The Earth's elliptical orbit causes variations in solar radiation received at the surface, with the distance ranging from approximately 147 million km at perihelion (closest point to the Sun) to 152 million km at aphelion (farthest point). These fluctuations lead to slight seasonal variations in the intensity of solar energy reaching the top of the atmosphere, even though the solar constant remains consistent. Atmospheric factors such as scattering, absorption, and reflection by clouds and air molecules further modify the solar radiation that ultimately reaches the Earth's surface. In addition, the angle of incidence of solar radiation on a given location varies depending on the latitude, time of day, and season, significantly affecting the amount of energy captured by solar panels. Optimal panel positioning and tilt angle adjustments are crucial to maximizing the utilization of this variable yet abundant resource. Reference Fig. 1.1 to visualize the Earth-Sun distance variation and its impact on solar energy reception.

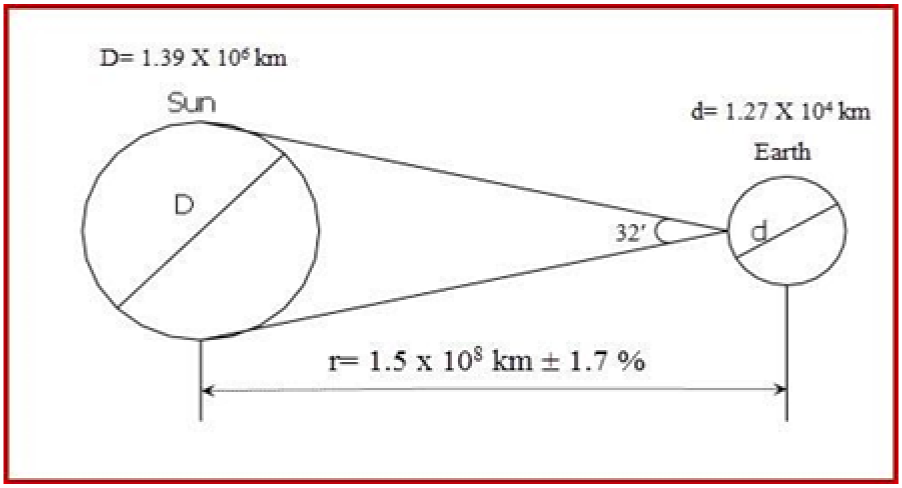

Figure 1.1 Variation in Sun-Earth Distance

Solar radiation passing through the Earth's atmosphere undergoes processes of absorption and scattering. A portion of this radiation is reflected back from the Earth's surface, re-entering the atmosphere and repeating these interactions.

The distribution of terrestrial and extraterrestrial zones contains various gases, such as nitrogen (N_2), carbon dioxide (CO_2), ozone (O_3), carbon monoxide (CO), oxygen (O_2), and water vapor (H_2O). These gases contribute to atmospheric absorption, while air molecules, dust particles, and water droplets are responsible for scattering radiation. Ozone and water vapor predominantly absorb ultraviolet radiation (wavelengths below 0.40 micrometres) and infrared radiation (wavelengths above 2.3 micrometres). In contrast, gases like nitrogen, oxygen, and others in the ionosphere absorb high-energy x-rays and extreme ultraviolet radiation from the Sun.

The atmosphere effectively absorbs most short-wave radiation with wavelengths below 0.29 micrometres. Consequently, the energy from solar radiation with wavelengths shorter than 0.29 micrometres or longer than 2.3 micrometres is minimal when it reaches the Earth's surface. Thus, solar radiation within the wavelength range of 0.29 to 2.3 micrometres is most significant for harnessing solar energy.

This selective absorption and scattering by the Earth's atmosphere significantly influence the spectral quality and intensity of solar radiation reaching the surface. The reduction in radiation intensity, known as atmospheric attenuation, varies depending on factors such as altitude, humidity, air pollution, and the angle of the Sun's rays. At higher altitudes or in less polluted regions, more solar energy reaches the ground due to reduced atmospheric interference.

Moreover, the greenhouse gases in the atmosphere, including carbon dioxide and water vapor, play a dual role. While they absorb and retain heat energy, contributing to the Earth's thermal balance, they also filter certain wavelengths of solar radiation. Understanding these interactions is crucial in solar energy systems design, as it determines the efficiency of photovoltaic cells and the effectiveness of concentrating solar power systems. By focusing on the usable spectrum of 0.29 to 2.3 micrometres, solar technology can maximize energy capture and utilization for sustainable energy solutions.

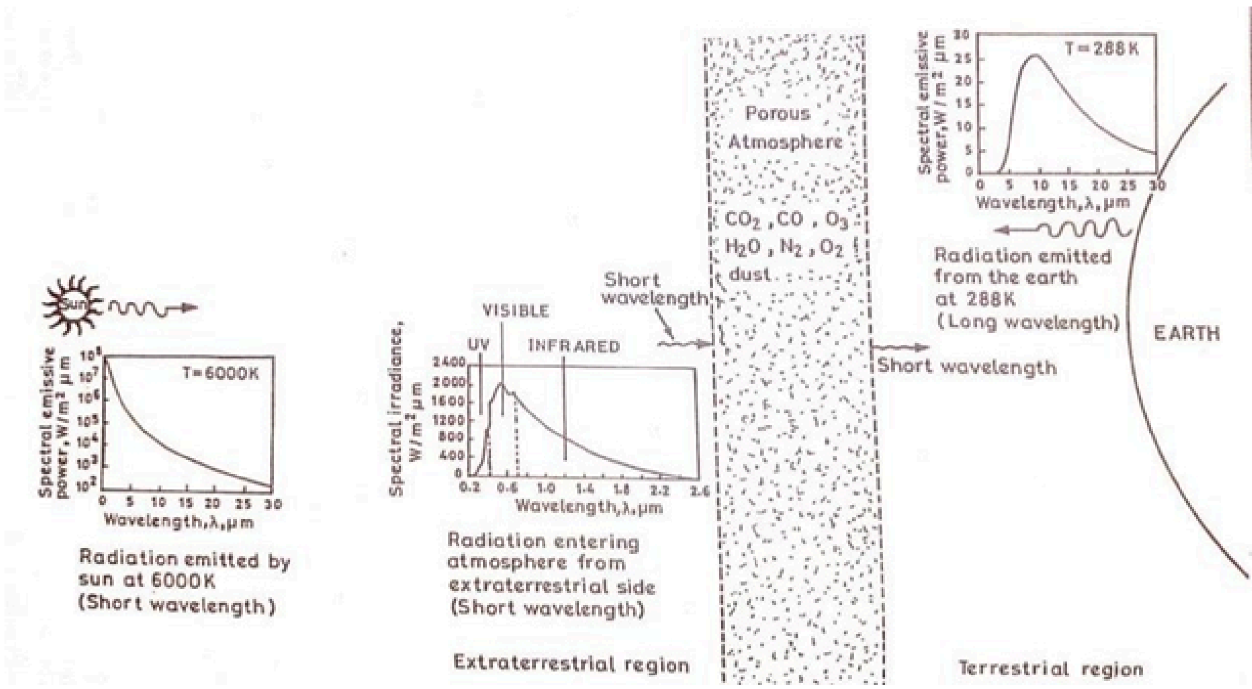

Figure 1.2: Propagation of Solar Radiation from the Sun to the Earth through the Atmosphere

1.3 Classification of Radiation and Related Terms

Beam Radiation: Solar radiation traveling directly along the line connecting the Sun and the receiving surface. This is also referred to as direct radiation.

Diffuse Radiation: Solar energy scattered by aerosols, dust particles, and atmospheric molecules. These rays lack a fixed direction and are not aligned with any specific path.

Global Radiation: Also known as total radiation, this is the sum of beam and diffuse radiation, commonly referred to as insolation.

Irradiance: The rate at which radiant energy is incident on a surface, measured per unit surface area.

Irradiation (Radiant Exposure): The total energy per unit area received by a surface, calculated by integrating irradiance over a specific period, such as an hour or a day. The term "insolation" is often used to describe solar energy irradiation.

Radiosity (Radiant Exitance): The rate at which radiant energy leaves a surface per unit area, resulting from the combined effects of emission, reflection, and transmission.

1.4 Sun-Earth Angles

The calculation of solar radiation involves various angles and parameters that significantly influence its variation.

Key angles include the solar zenith angle, solar altitude angle, and solar azimuth angle, which collectively define the Sun's position relative to a specific location on Earth. The solar zenith angle is the angle between the Sun's rays and the vertical direction at a given point, while the solar altitude angle represents the Sun's height above the horizon.

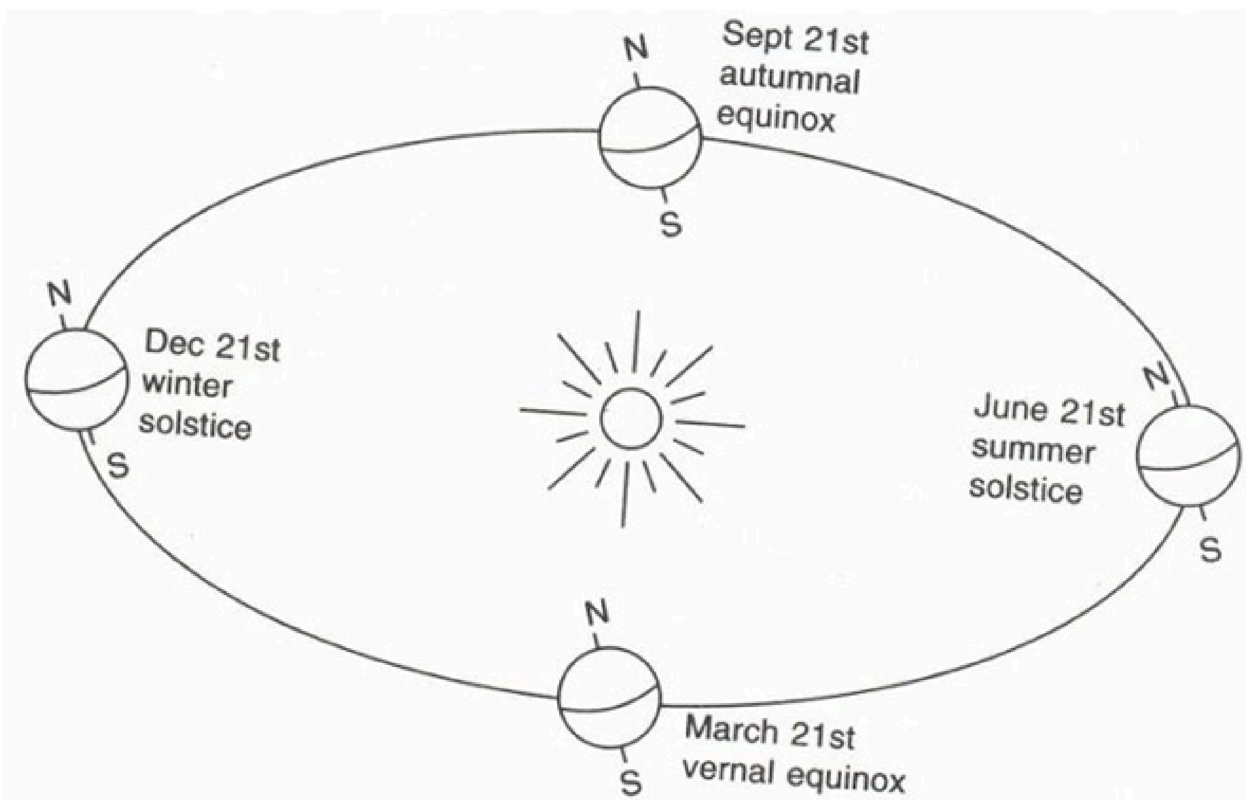

Figure 1.3: Solar Geometry

The following predefined angles play a crucial role in determining solar radiation:

1.4.1 Angle of Incidence

The angle of incidence refers to the angle formed between the Sun's radiation and the surface's normal. Its value depends on all the other angles defined below. Please take reference from Fig. 1.4

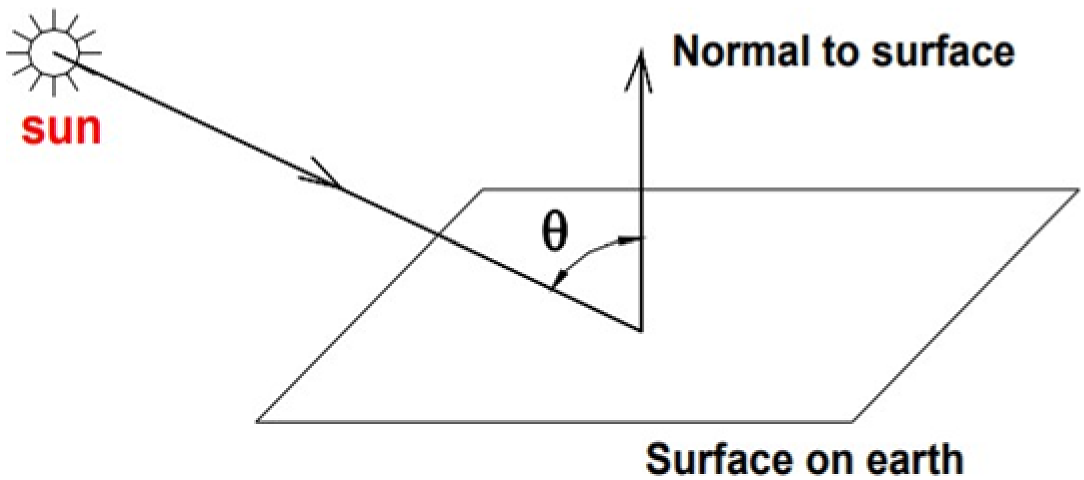

Figure 1.4: Angle of Incidence

1.4.2 Zenith Angle

For a horizontal surface, the zenith angle is the angle between the surface's normal and the Sun's radiation. On horizontal planes, the angle of incidence equals the zenith angle.

The zenith angle varies throughout the day as the Sun moves across the sky and is influenced by the observer's geographical latitude, the time of year, and the Earth's axial tilt. At solar noon, when the Sun is at its highest point in the sky, the zenith angle is at its minimum, directly affecting the intensity of solar radiation received.

For locations on the equator during an equinox, the zenith angle at solar noon is zero, meaning the Sun is directly overhead. However, for higher latitudes or during solstices, the zenith angle increases, reducing the solar energy received due to the oblique incidence of sunlight. Refer Fig. 1.5 to understand better.

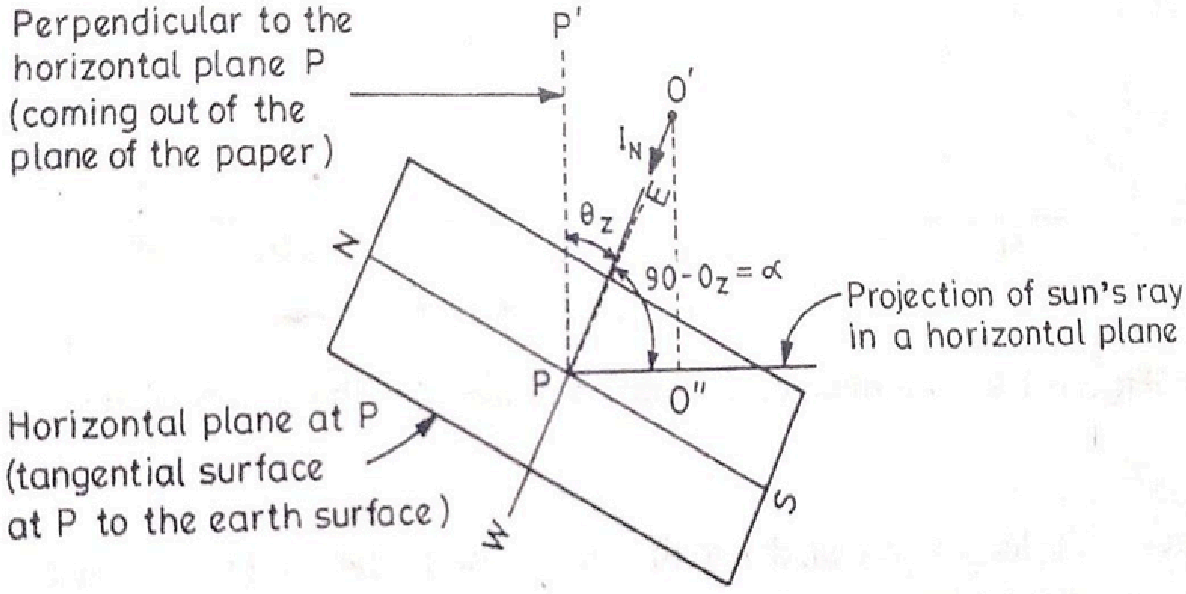

Figure 1.5: Zenith Angle

1.4.3 Latitude Angle

Latitude represents a location's position on Earth. It is defined as the angle between the radial line connecting the specified location to the Earth's center and its projection on the equatorial plane. Latitude is positive in the northern hemisphere and negative in the southern hemisphere.

1.4.4 Declination

Declination is the angle formed between the line connecting the Sun and Earth's centers and its projection onto the equatorial plane. It results from the Earth's axial tilt of 66.5° relative to the plane of its orbit around the Sun.

The variation in declination throughout the year is a consequence of the Earth's elliptical orbit and axial tilt, leading to the phenomenon of seasons. On the equinoxes (around March 21 and September 21), the declination angle is zero, meaning the Sun is directly above the equator, resulting in nearly equal day and night durations globally.

During solstices, the maximum declination of +23.45° (June 21) aligns the Sun directly over the Tropic of Cancer, while the minimum declination of -23.45° (December 21) positions it over the Tropic of Capricorn. This cyclical change in declination is crucial for calculating solar angles, such as altitude and azimuth, and plays a pivotal role in designing solar energy systems, as it directly affects the solar radiation incident on a surface. Refer Fig. 1.6

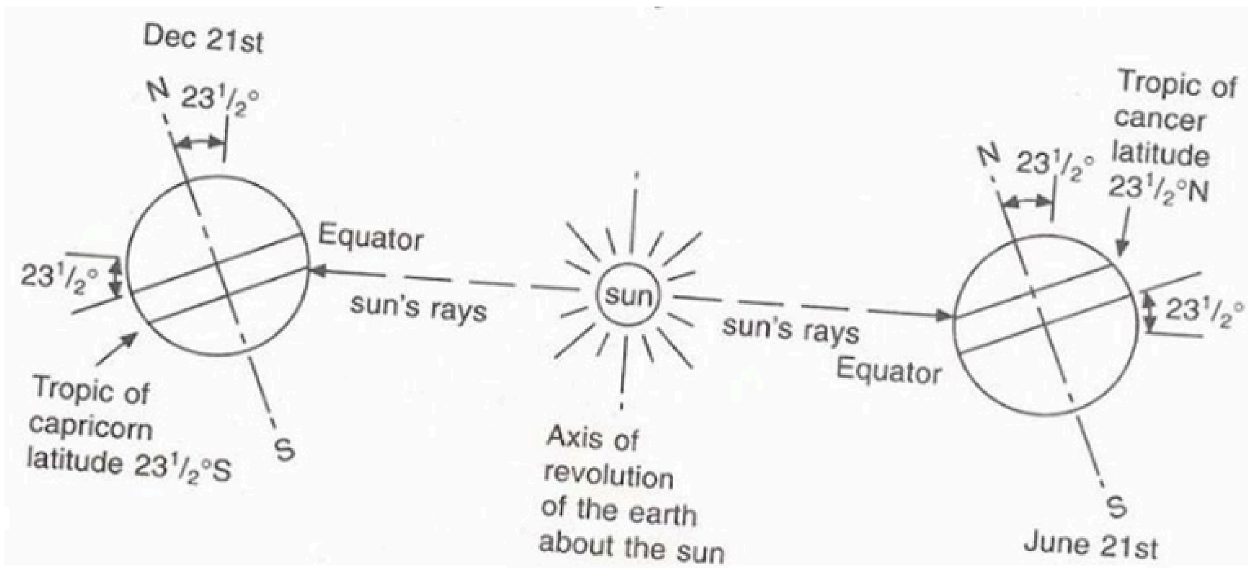

Figure 1.6: Angle with Respect to Earth's Rotation

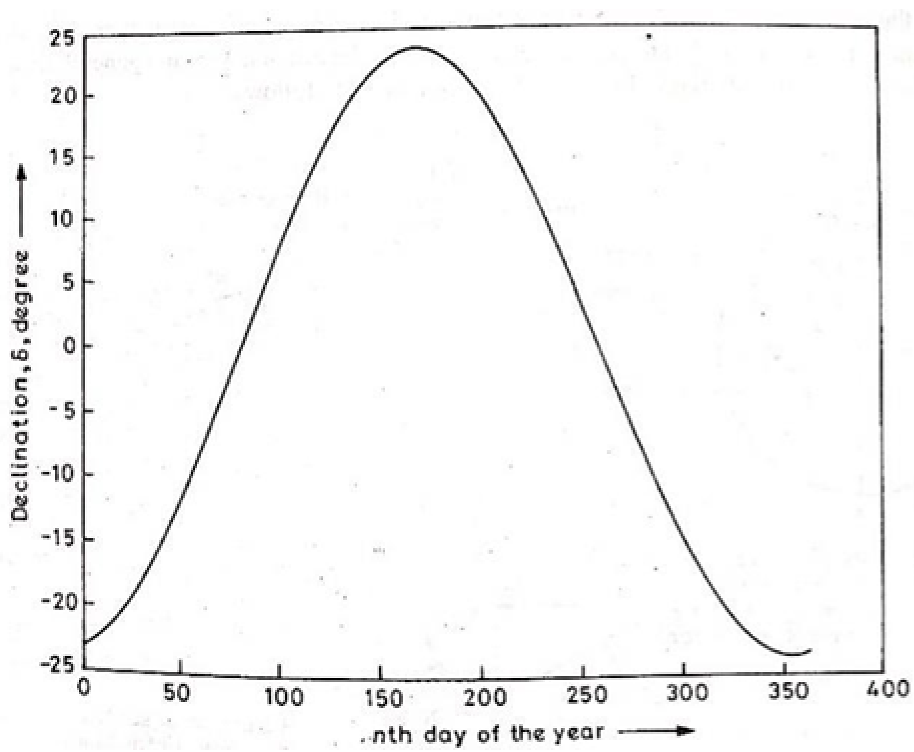

Figure 1.7: Variation of Declination Angle Over the Year

1.4.5 Hour Angle

The hour angle represents the angular displacement of the Sun east or west of the local meridian due to the Earth's rotation at 15° per hour. It is zero at solar noon, negative in the morning, and positive in the afternoon for the northern hemisphere, with the opposite pattern for the southern hemisphere.

1.4.6 Altitude Angle

The altitude angle is the angle formed by the Sun's rays with a horizontal surface. It is the complement of the zenith angle and reaches its maximum value at solar noon.

1.4.7 Solar Azimuthal Angle

This is the angle in the horizontal plane between the line due south and the horizontal projection of the Sun's rays. For the northern hemisphere, the angle is positive if the projection is east of south and negative if west of south, and vice versa for the southern hemisphere.

1.4.8 Slope (Tilt Angle)

The slope, or tilt angle, is the angle between a surface and the horizontal plane. It is positive for surfaces sloping southward and negative for those sloping northward.

1.4.9 Surface Azimuthal Angle

Table 1.1: Surface Azimuthal Angle for Various Orientations in the Northern Hemisphere

Surface Orientation	**Azimuthal Angle (ϒ)**
Tilted towards South	**0°**
Tilted towards North	**-180°**
Tilted towards East	**-90°**
Tilted towards West	**+90°**
Tilted towards Southeast	**-45°**
Tilted towards Southwest	**+45°**

Refer Table 1.1. The surface azimuthal angle is the angle in the horizontal plane between the line due south and the projection of a surface's normal (inclined plane) onto the horizontal plane. For the northern hemisphere, it is negative if the projection is east of south and positive if west of south, with the convention reversed in the southern hemisphere.

In practice, the surface azimuthal angle helps identify how sunlight strikes an inclined surface throughout the day, influencing the incident angle of solar radiation. Combined with the tilt angle, it provides a complete description of the surface's orientation. Adjusting this angle, especially in solar tracking systems, can significantly enhance energy production by aligning the panels more directly with the Sun's rays during peak sunlight hours. A proper understanding of this angle is crucial for optimizing the tilt and orientation of solar panels, particularly in systems where maximum energy capture is desired. It is critical for the efficiency of photovoltaic systems and solar thermal applications.

Solar Wall Azimuthal Angle

The solar wall azimuthal angle refers to the angle formed between the normal to an inclined plane and the projection of the Sun's rays on a horizontal plane. All these parameters vary as the Earth's orientation changes relative to the Sun.

1.5 Climatic Classification

Climatic classification is primarily based on variations in temperature and the moisture content in the air. India has six distinct climatic zones, described as follows:

1.5.1 Subtropic Arid Climatic Zone

This zone is characterized by potential evaporation exceeding precipitation, resulting in constant water deficiency. For this study, Bikaner, Rajasthan, has been selected as the representative city.

1.5.2 Tropical Rainforest Climatic Zone

Regions in this zone experience abundant rainfall, and the temperature of the coldest month does not fall below 18°C. Guwahati, Assam, has been chosen as the representative city. This region is characterized by a tropical monsoon climate, with high humidity levels and significant seasonal variations in rainfall.

1.5.3 Mountain Climatic Zone

High solar insolation, low temperatures, low pressure, significant precipitation, and large diurnal temperature variations are typical of these regions, especially at higher altitudes. Kargil, Ladakh, is the selected city for this zone.

1.5.4 Subtropical Semi-Arid Climatic Zone

In this zone, the temperature of the coldest month is below -3°C, while the warmest month sees temperatures above 10°C. Amritsar, Punjab, represents this region.

1.5.5 Tropical Semi-Arid Climatic Zone

This zone experiences heavy rainfall along with dry seasons. Bangalore, Karnataka, has been selected as the representative city.

1.5.6 Tropic Wet and Dry Climatic Zone

Regions in this zone generally experience warm temperatures and regular rainfall. Raipur, Chhattisgarh, represents this climatic condition.

1.6 ASHRAE Model (Clear Sky Conditions)

The **ASHRAE Model**—developed by the *American Society of Heating, Refrigerating, and Air-Conditioning Engineers*—is an empirical model used to calculate total solar irradiation on a horizontal surface. The model incorporates three climatic constants whose values depend on the specific day of the year.

The methodology involves first estimating total solar irradiation on a horizontal surface, followed by applying specific factors to calculate the solar irradiation on an inclined surface.

Key Parameters:

- **θ**: Incidence Angle
- **δ**: Declination Angle
- **γ**: Surface Azimuthal Angle
- **β**: Tilt Angle
- **ω**: Hour Angle

CHAPTER – II

LITERATURE REVIEW

The literature review presents several studies that focus on estimating solar radiation using different models, with a particular emphasis on the ASHRAE clear-sky model. Omar Behar et al. [1] evaluated 17 clear-sky models in Algeria and identified ASHRAE as the most accurate for Direct Normal Irradiance (DNI). Similarly, Sami A. Al-Sanea [2] validated the ASHRAE model in Riyadh, recommending adjustments for cloudiness factors. Other studies, like those by B. Jamil [3] and Christian A. Gueymard et al. [4], further validated the model's efficiency in various climates, including India and Mediterranean regions. Additionally, Pansak Amarananwattana et al. [5] and N. N. Nizhegorodov et al. [6] modified the ASHRAE model to account for local atmospheric conditions, improving its accuracy for regions with high humidity and low aerosol presence. Overall, these studies show the widespread application of the ASHRAE model in estimating solar radiation, with adjustments tailored to specific environmental conditions for better accuracy.

Omar Behar et al. [1]

Omar Behar and colleagues highlighted the importance of estimating direct solar radiation for solar energy projects, particularly in regions lacking aerial or radiometric monitoring stations. They evaluated the efficiency of 17 clear-sky solar radiation models for Algeria's climate, using Ghardaia irradiance measurements. Their assessment employed the Global Performance Indicator validation method, along with a new statistical accuracy indicator to identify the most precise models. By comparing projected values with frequent measurements at Ghardaia, they tested six statistical indicators assessing each model's linearity, short- and long-term performance, and modeling proficiency. Among the models, ASHRAE consistently outperformed others, offering more accurate Direct Normal Irradiance (DNI) data.

Sami A. Al-Sanea [2]

Sami A. Al-Sanea used observational data from Riyadh, Saudi Arabia, to evaluate the ASHRAE clear-sky model. He calculated daily total solar flux by integrating hourly distributions and introduced a "cloudiness factor" for monthly adjustments, accounting for regional weather conditions. When the ASHRAE model estimates were modified using these factors, they aligned closely with measured monthly average hourly solar flux values. The study recommends applying these corrections to calculate solar radiation in Riyadh and similar climates. The findings validated the ASHRAE model's predictions, especially from October to May, making it suitable for solar energy applications, such as building energy analysis, in Riyadh’s climate.

B. Jamil [3]

B. Jamil applied the ASHRAE clear-sky model to determine solar radiation under clear-sky conditions in Aligarh, India. The study concluded that the ASHRAE model is a quick and efficient tool for analyzing solar radiation on various surfaces, including solar collectors and photovoltaic panels. Additionally, the model facilitates separate calculations for radial and diffuse components of global solar radiation.

Christian A. Gueymard et al. [4]

Christian A. Gueymard and co-authors evaluated 54 broadband models for estimating global and diffuse solar radiation on horizontal surfaces. Their research concluded that no single model is universally optimal. However, ESRA3, Ineichen, METSTAT, and REST2 ranked as top models for global solar radiation estimation, while Bird, CEM, and Paulescu & Schlett were recognized as secondary options. For diffuse solar radiation, the King and ASHRAE2005 models emerged as the most accurate.

Pansak Amarananwattana et al. [5]

Pansak Amarananwattana utilized the ASHRAE clear-sky model to calculate solar heat loads in architectural and engineering applications under Thai atmospheric conditions. The study noted significant differences between Thai and U.S. atmospheres, prompting adjustments to ASHRAE model parameters. Using five years of sunny-day solar radiation data, they modified the model to improve its accuracy. The findings revealed that the Root Mean Square Error (RMSE) for unadjusted ASHRAE models was about 64%, 37%, and 15% for diffuse, direct, and global radiation, respectively, in Upper Thailand. In Southern Thailand, these errors were 60%, 19%, and 7%. High humidity and low aerosol presence contributed to model biases, which were mitigated through parameter adjustments.

N. N. Nizhegorodov et al. [6]

N. N. Nizhegorodov and team used the empirical A, B, and C coefficients of the ASHRAE model to compute solar radiation for sunny days. They analyzed various radiation components and found that low humidity, low turbidity, and small relative air mass values led to higher direct normal solar irradiation during sunrise and sunset.

Using the empirical coefficients, they developed hourly and daily solar radiation forecasts based on isotropic and anisotropic sky models, along with revised relative air mass formulas. Their work also included creating a computer program for ground and atmospheric radiation predictions.

S. BARO, G. CANNISTRARO, et al. [7]

S. Baro and G. Cannistraro applied the GL Powell-proposed ASHRAE clear sky model to analyze Palermo’s annual solar radiation data at short time intervals. The results revealed that the model's computed values were generally higher than measured data. To address this, they recalculated and proposed new atmospheric extinction coefficients suitable for the Mediterranean climate. The ASHRAE model factors in water vapor, ozone, and dust. However, while the water vapor levels in Palermo stayed within the ASHRAE-defined range, ozone levels in the Mediterranean frequently exceeded the model's 2.5 mm estimate.

Dr. Didier Thévenard et al. [8]

Dr. Didier Thévenard and colleagues updated the ASHRAE climatic data for design standards, concluding that the model provides a simple and effective way to calculate solar radiation components using location-specific parameters. This is particularly useful for determining building cooling loads. The 2009 version of the ASHRAE clear-air solar radiation model was revised in 2013 to include improved aerosol data and a refined compression model. The updates were validated through statistical analysis using clear-sky solar radiation data from multiple radiometric stations, resulting in a more accurate model with variable aerosol and compositional factors.

Khalida, Muhammad Zakaria, et al. [9]

Khalida and Muhammad Zakaria estimated solar radiation in southern Pakistan by analyzing five models: temperature-based, cloud-based, meteorological-based, geographic-based, and combined meteorological-geographic models. They assessed the models using mean prediction errors and Theil inequality coefficients. The study found that models incorporating meteorological and topographical parameters were the most accurate for estimating solar radiation in Pakistan.

M. Jamil Ahmad and G. N. Tiwari [10]

M. Jamil Ahmad and G. N. Tiwari utilized the ASHRAE model with updated A, B, and C constants to estimate hourly solar radiation and atmospheric scattering in India.

They categorized days based on diffuse radiation and daylight hours:
(a) Clear/blue sky: Diffuse radiation < 25% of total, >9 hours daylight.
(b) Partly cloudy: Diffuse radiation 25-50%, 7-9 hours daylight.
(c) Foggy/cloudy: Diffuse radiation 50-75%, 5-7 hours daylight.
(d) Fully cloudy: Diffuse radiation >75%, <5 hours daylight.
Their findings demonstrated the model's effectiveness in estimating solar irradiance across varied conditions.

Y. El Moghouchi et al. [11]

Y. El Moghouchi and co-authors conducted statistical analyses across 24 Moroccan cities to evaluate the ASHRAE model's daily performance. Their results showed strong approximations between calculated and measured values, particularly under clear-sky conditions, enhancing daily solar radiation intensity predictions.

L.T. Wong, W.K. Zhou, et al. [12]

L.T. Wong and W.K. Zhou compared seven solar irradiance models to forecast daily and hourly global, radiant, and diffuse irradiance. The study identified limitations in the ASHRAE model due to its outdated solar constant (1322 W/m²) and use of older spectral irradiance data. The model also failed to account for surface albedo, affecting its accuracy for diffuse radiation predictions.

Western, B.E. [13]

Western analyzed solar radiation in New Zealand using the ASHRAE Clear Sky Radiation Model and local meteorological data. The updated parameters demonstrated strong correlations between measured and estimated values for both horizontal and vertical planes. The revised ASHRAE model, combined with the Gracefield parameter, provided accurate clear-sky radiation estimates for solar installations.

K.J. Kontoleon et al. [14]

K.J. Kontoleon introduced an improved thermal network-based dynamic modeling approach for buildings, integrating the ASHRAE clear-sky model to calculate solar radiation on façades. Their simulations in Mediterranean regions showed the significance of façade orientation and glazing systems in reducing energy consumption. Results aligned with reported monthly radiation data for different surface orientations.

REN Zhi Gang [15]

Ren Zhi Gang compared the ASHRAE, Hottel, and Digler models to evaluate solar irradiation's impact on bridge temperature fields. The study found the ASHRAE model most effective when sufficient solar observation data was available to refine its parameters.

Samer Alsadi et al. [16]

Samer Alsadi modified the ASHRAE model parameters to suit Arab countries' meteorological conditions. Using RMSE, MBE, and t-stat analyses, the improved model demonstrated strong accuracy in predicting global solar irradiance across cities like Riyadh, Palestine, and Libya. The refined A, B, and C parameters enhanced the model's usability without requiring extensive input data.

Mohamed Abouhashish et al. [17]

Mohamed Abouhashish applied the ASHRAE clear-sky model in Saudi Arabia and observed high hourly beam radiation predictions but low hourly diffuse radiation. Using Microsoft Visual Basic, they developed a simulation model for solar geometry and introduced factors to compare measured DNI and DHI values against the model. The findings suggested the ASHRAE model effectively estimates monthly radiation components, though daily profiles showed slight deviations.

V. Maslensky et al. [18]

V. Maslensky examined heat loads from solar radiation on mobile machine cabins using the ASHRAE model integrated with ANSYS FLUENT. Their tailored approach for glazing-specific solar factors ensured accurate temperature control system assessments, highlighting the model's adaptability for automated calculations.

CHAPTER – III

METHODOLOGY

This chapter outlines the methodology employed to compute the solar irradiation falling on a surface and optimize the tilt angle for maximum radiation. The process begins with defining essential inputs such as location latitude, day of the year, surface azimuth angle, and reflectivity. It incorporates precise calculations like declination, solar radiation parameters, and view factors. A programming algorithm systematically evaluates these inputs using iterative loops and mathematical formulas to calculate key parameters, including zenith and inclination angles. Finally, the methodology optimizes the tilt angle to achieve maximum radiation, ensuring an efficient solar energy analysis.

Programming Algorithm

To calculate the irradiation falling on a surface, the following inputs are required:

1. **Latitude of the Location** :
    1.1) Enter latitude in degrees (user input).
    1.2) Convert latitude to radians for mathematical calculations.
2. **Day of the Year (N)** :
    2.1) Input the day number corresponding to the desired date.
    For example:
    January 21 = 21
3. **Surface Azimuth Angle (sa)**:
    3.1) Determine the wall's orientation based on user input:
    South-facing: sa = 0sa = 0
    North-facing: sa = 180sa = 180
    East-facing: sa = −90sa = -90
    West-facing: sa = 90sa = 90
4. **Hour Angles**:
    4.1) Define an array of hour angles from 9:00 AM to 4:00 PM at 30-minute intervals. Example:
    9:00 AM: w = 45 w = 45
    9:30 AM: w = 37 w = 37
5. **Reflectivity**:
    5.1) Set reflectivity to ρ = 0.6
6. **Initial Tilt Angle (t)**:

    6.1) Start with a tilt angle of t = 90

Computation

Step 1: Calculate Declination (d)

Declination (d) = 23.47 **×** sin(360(284+N)/365)

where d = declination in radian

Step 2: Compute View Factors

View factors

fws1 = (1+cosβ)/2

fwg1 = ρ×(1-cosβ)/2

Step 3: Define Solar Radiation Parameters

- AA: Solar irradiance beyond the atmosphere.
  AA = 1162.12+77.0323 × cos (d×360/365)
- BB: Atmospheric extinction coefficient.
  BB = 0.171076−0.0348944 × cos (d×360/365)
- CC: Diffuse radiation factor.
  CC = 0.0897334−0.0412439 × cos(d×360/365)

Step 4: Iterative Calculations for Hour Angles

- Run a loop for 15 hour angles.
- For each hour angle ww:
  - Computing zenith angle
    (za1) = cos-1(sinφ × sinδ + cosφ × cosδ × cosω)
  - Adjust zenith angle if θz > 90◦
    & θz > 90◦
    θz = θz − 90◦
  - Compute inclination angle (θ):

    cosθ = (sinφ × sinδ × cosβ + cosδ × cosϒ × cosω × sinβ + cosφ × cosδ × cosϒ × cosβ − sinδ × cosω × sinϒ +cosδ × sinϒ × sinω × sinβ)

- Adjust inclination angle if $\theta > 90^\circ$:

  $\theta = \theta - 180^\circ$

Step 5: Radiation Calculations

- Beam radiation ratio:
  $rb = (\cos\theta / \cos(\theta z))$

- Direct radiation:
  Direct radiation (IDN)= $A.\exp(-B\cos(\theta z))$

- Diffuse radiation (Id):
  Diffused radiation (Id)= $C \times IDN$

- Direct radiation on the wall (Ib):
  Direct radiation on the wall (Ib)= $IDN \times \cos(\theta z)$

Step 6: Total Radiation (It)

Total radiation (It)= $IB \times RB + ID \times Fws + (IB+ID) \times FWG$

- Store total radiation values for each hour angle.
- Find the maximum radiation
- Record the hour angle corresponding to maximum radiation.

Step 7: Tilt Angle Optimization

- For the hour angle with maximum radiation, iterate over different tilt angles to identify the optimal tilt for maximum radiation.

Step 8: Repeat Entire Process

- Recalculate total radiation for new conditions and optimize tilt angles.

CHAPTER – IV

RESULTS

This section examines the monthly variation in the optimum tilt angle for solar panels across six distinct cities. By comparing the radiation values for each city during winter and spring, the study highlights the regional differences and the significant improvements in solar energy efficiency achieved through optimizing tilt angles. This analysis provides valuable insights for designing effective solar power systems tailored to local geographic and seasonal conditions.

4.1 Monthly Variation of Optimum Tilt Angle Across Six Cities

Figures: Variation of Optimum Tilt Angle for Six Different Cities

In winter, on December 21st at 12 PM, the variation in solar radiation is quite noticeable between different regions. Bangalore, benefiting from a 30° tilt, achieves the highest total solar radiation of 1337.64 W/m², which is optimal for this date. In contrast, Srinagar experiences the lowest solar radiation at 1151.63 W/m², recorded on a flat surface, indicating a significant reduction in efficiency without tilting.

For Bikaner, as explained in Fig 4.1 the optimal tilt angle for maximum solar radiation during winter is 51°, with the total radiation reaching 1218.75 W/m². This is compared to the average tilt angle of 30°, which results in radiation of 1149.75 W/m².

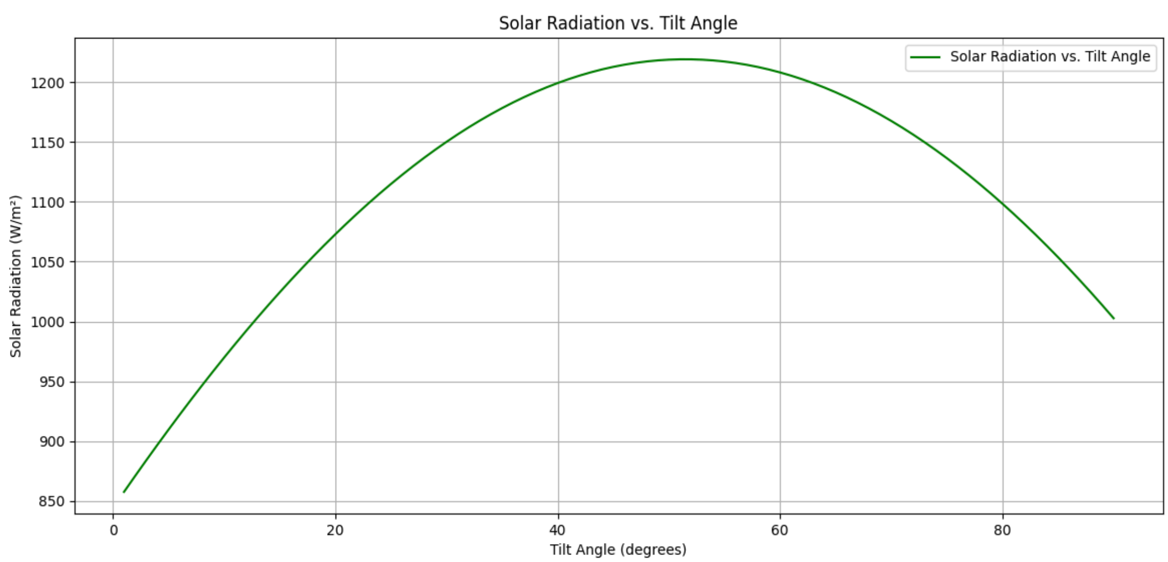

Figure 4.1: Variation of Optimum Tilt Angle for Bikaner (Winter)

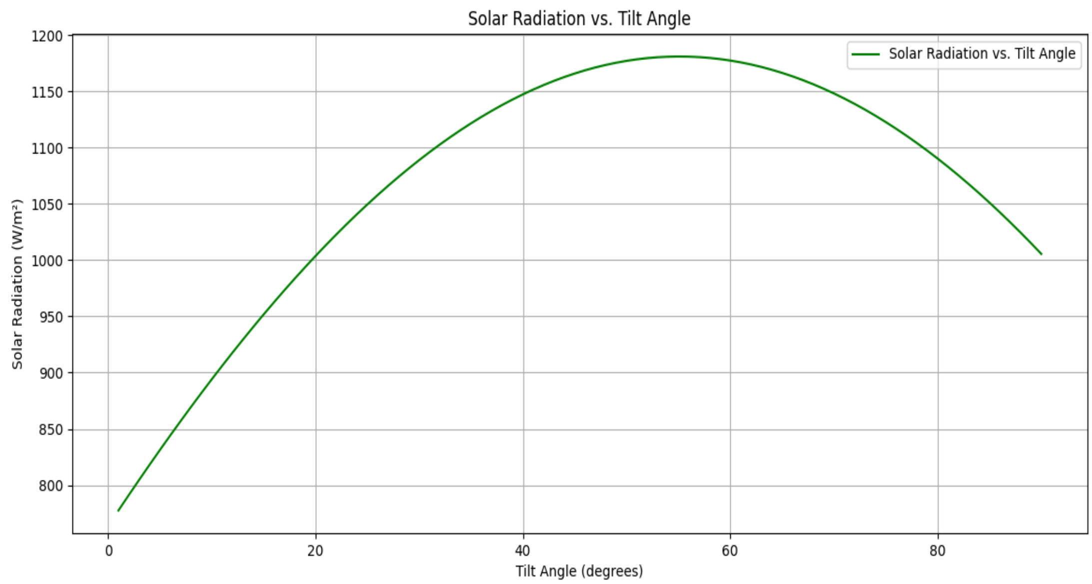

Figure 4.2 : Variation of Optimum Tilt Angle for Amritsar (Winter)

For Amritsar, as explained in Fig 4.2, the optimal tilt angle for maximum solar radiation during winter is 55°, with the total radiation reaching 1180.49 W/m². In comparison, at a standard tilt angle of 30°, the solar radiation decreases to 1088.40 W/m², indicating a notable increase in energy capture by adjusting the tilt angle to 55°.

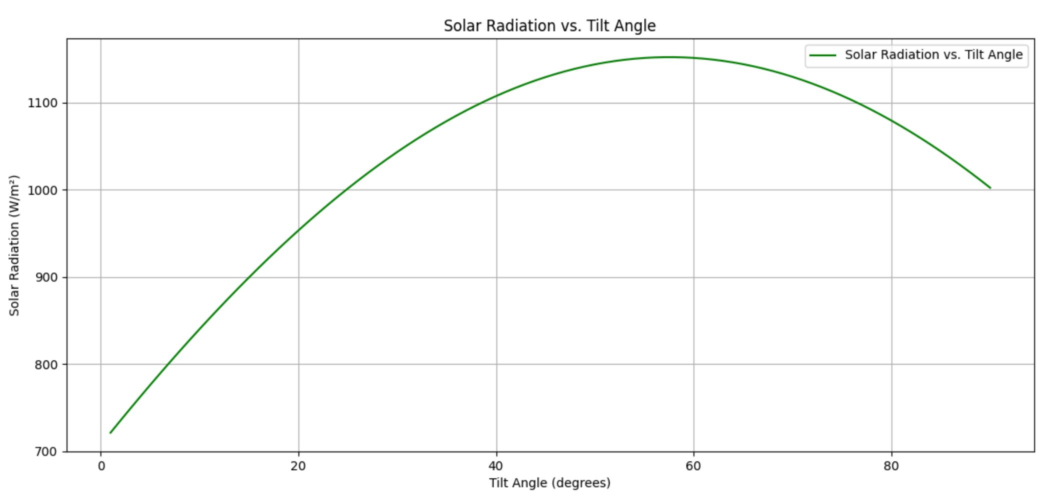

Figures 4.3: Variation of Optimum Tilt Angle for Srinagar (Winter)

For Srinagar, as explained in Fig 4.3 the optimal tilt angle for maximum solar radiation during winter is 58°, yielding a total radiation of 1151.62 W/m². When the solar panels are tilted at the average angle of 30°, the radiation decreases to 1042.8 W/m².

For Bangalore, as explained in Fig 4.4, the optimal tilt angle for maximum solar radiation during winter is 36°, resulting in a total radiation of 1337.63 W/m². In contrast, when the solar panels are tilted at the average angle of 30°, the radiation is slightly lower at 1331.07 W/m².

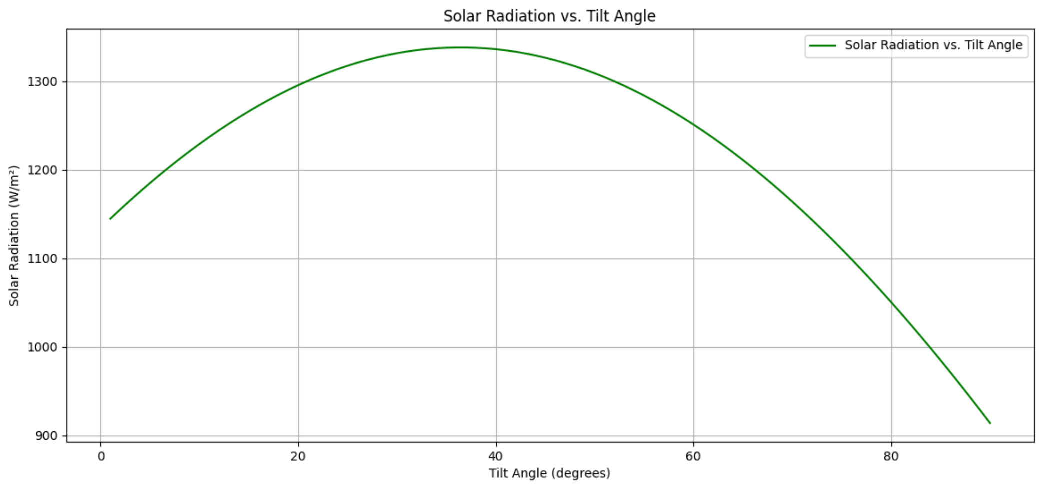

Figures 4.4: Variation of Optimum Tilt Angle for Bangalore (Winter)

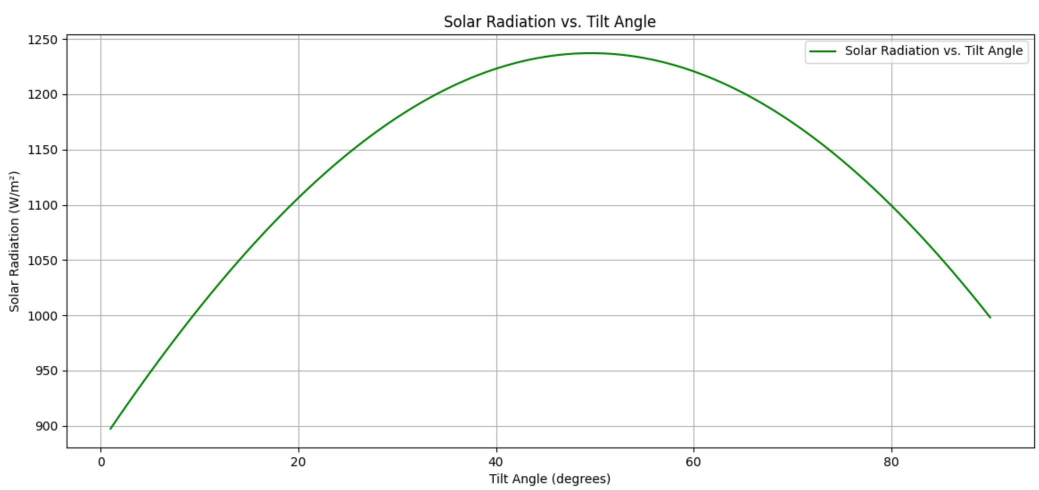

Figures 4.5: Variation of Optimum Tilt Angle for Guwahati (Winter)

For Guwahati, as explained in Fig 4.5, the optimal tilt angle for maximum solar radiation during winter is 50°, resulting in a total radiation of 1236.76 W/m². When the solar panels are tilted at the average angle of 30°, the radiation decreases to 1178.62 W/m². This difference highlights the advantage of adjusting the tilt angle to 50° to maximize solar energy collection, improving the efficiency of solar power systems in the region.

For Raipur, as explained in Fig 4.6, the optimal tilt angle for maximum solar radiation during winter is 45°, with a total radiation of 1279.16 W/m². In comparison, when the solar panels are tilted at the average angle of 30°, the radiation reduces to 1245.65 W/m².

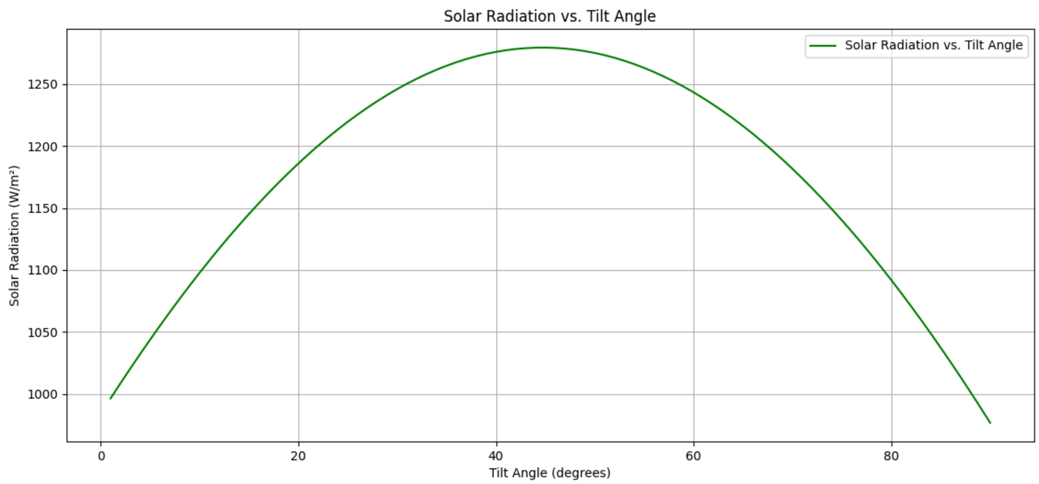

Figure 4.6: Variation of Optimum Tilt Angle for Raipur (Winter)

The percentage reduction in maximum solar radiation between Bangalore and other cities is as follows:

- Srinagar:13.9% (186 W/m²)
- Raipur: 4.3% (58 W/m²)
- Bikaner: 8.9% (119 W/m²)
- Amritsar: 11.7% (157 W/m²)
- Guwahati: 7.5% (101 W/m²)

Figures: Change in Optimum Tilt Angle During the Year

In Spring, on March 21st, Bangalore again receives the highest radiation (1349.12 W/m²) at a tilt of 25°, while Srinagar records the lowest (1265.64 W/m²) at 34°. The optimum tilt angles for various zones are:

For Bikaner, as explained in Fig 4.7, the optimal tilt angle for maximum solar radiation during spring is 28°, with the total radiation reaching 1297.80 W/m². This is compared to the average tilt angle of 30°, which results in a solar radiation of 1297.45 W/m², showing only a slight difference in radiation.

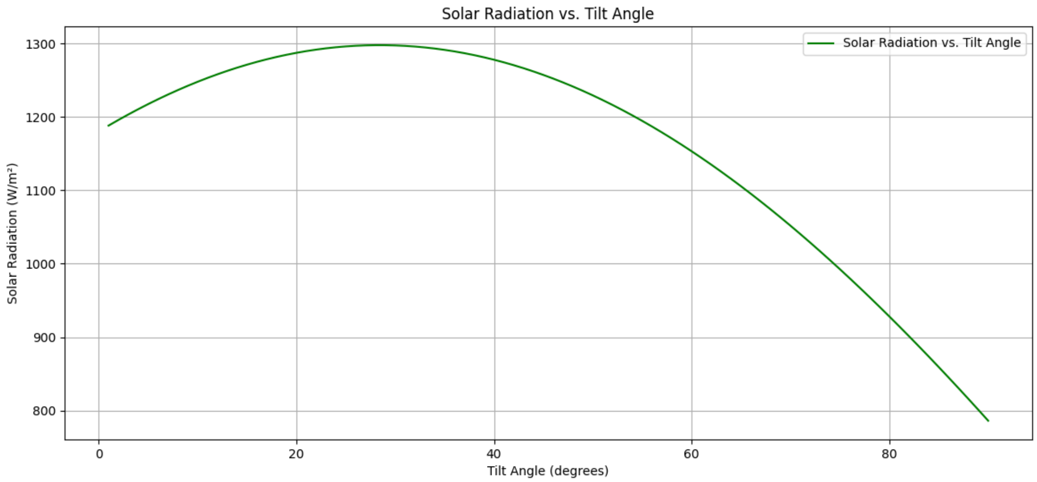

Figure 4.7: Variation of Optimum Tilt Angle for Bikaner (Spring)

For Amritsar, as explained in Fig 4.8, the optimal tilt angle for maximum solar radiation during spring is 32°, with the total radiation reaching 1279.50 W/m². This is compared to the average tilt angle of 30°, which results in a solar radiation of 1278.88 W/m², showing a very slight difference in radiation. While the difference is minimal, this emphasizes the need to carefully consider the optimal tilt angle to maximize solar energy collection and improve system efficiency. This marginal difference highlights that even small adjustments in tilt angle can contribute to improved solar energy yield, underscoring the importance of precision in solar panel installation for optimal performance in different regions.

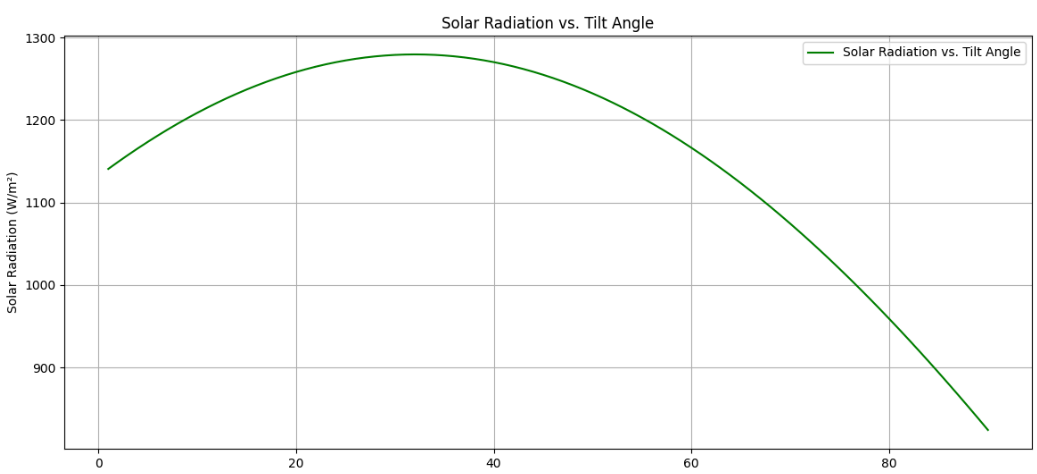

Figure 4.8: Variation of Optimum Tilt Angle for Amritsar (Spring)

For Srinagar, as explained in Fig 4.9, the optimal tilt angle for maximum solar radiation during spring is 34°, with the total radiation reaching 1265.65 W/m². In comparison, at an average tilt angle of 30°, the solar radiation decreases slightly to 1262.72 W/m².

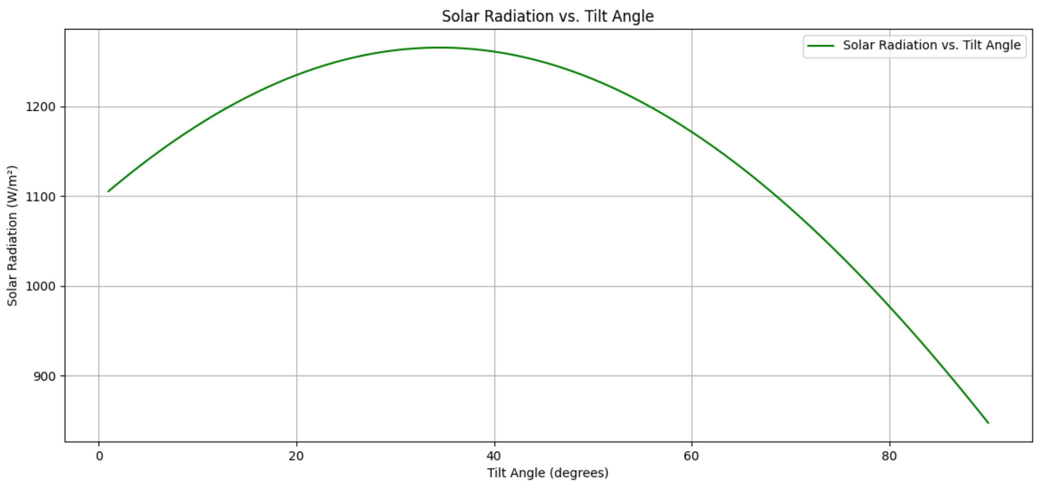

Figure 4.9: Variation of Optimum Tilt Angle for Srinagar (Spring)

For Bangalore, as explained in Fig 4.10, the optimal tilt angle for maximum solar radiation during spring is 13°, with the total radiation reaching 1349.13 W/m². In comparison, at an average tilt angle of 30°, the solar radiation decreases to 1307.6 W/m². This difference highlights the importance of adjusting the tilt angle to local conditions, as even a small variation can result in a noticeable increase in solar energy capture.

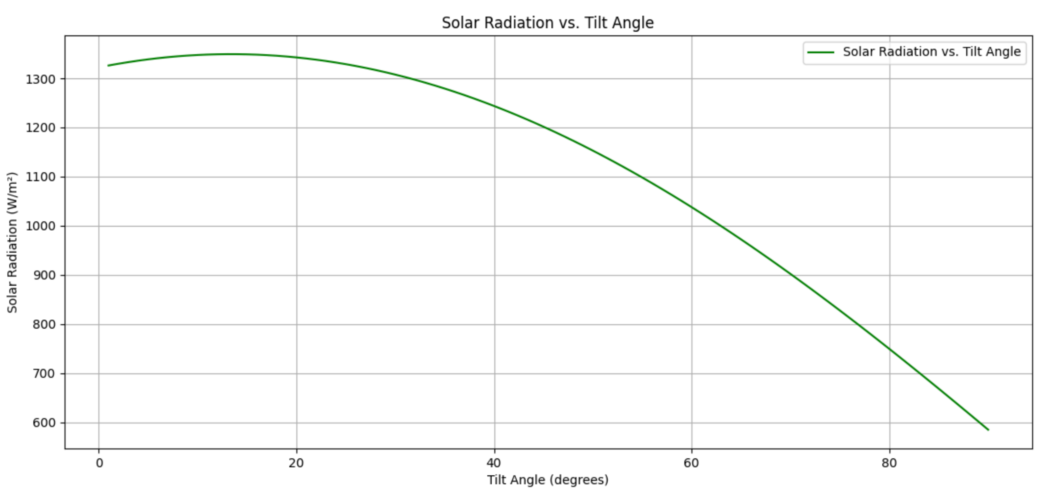

Figure 4.10: Variation of Optimum Tilt Angle for Bangalore (Spring)

For Guwahati, as explained in Fig 4.11, the optimal tilt angle for maximum solar radiation during the spring season is 27°, yielding a total radiation of 1306.30 W/m². In comparison, at the average tilt angle of 30°, the radiation is slightly lower at 1304.45 W/m², demonstrating that even small adjustments in tilt angle can lead to improved solar energy capture in different regions.

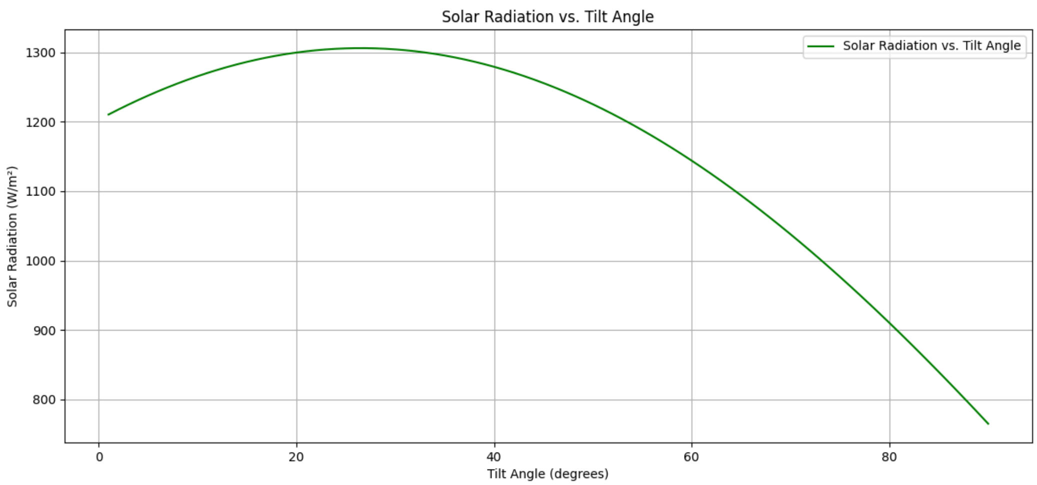

Figure 4.11: Variation of Optimum Tilt Angle for Guwahati (Spring)

For Raipur, as explained in Fig 4.12, the optimal tilt angle for maximum solar radiation during the spring season is 22°, with a total radiation of 1325.66 W/m². At the average tilt angle of 30°, the radiation decreases slightly to 1315.23 W/m², indicating that adjusting the tilt angle closer to 22° can enhance solar energy collection efficiency in this region.

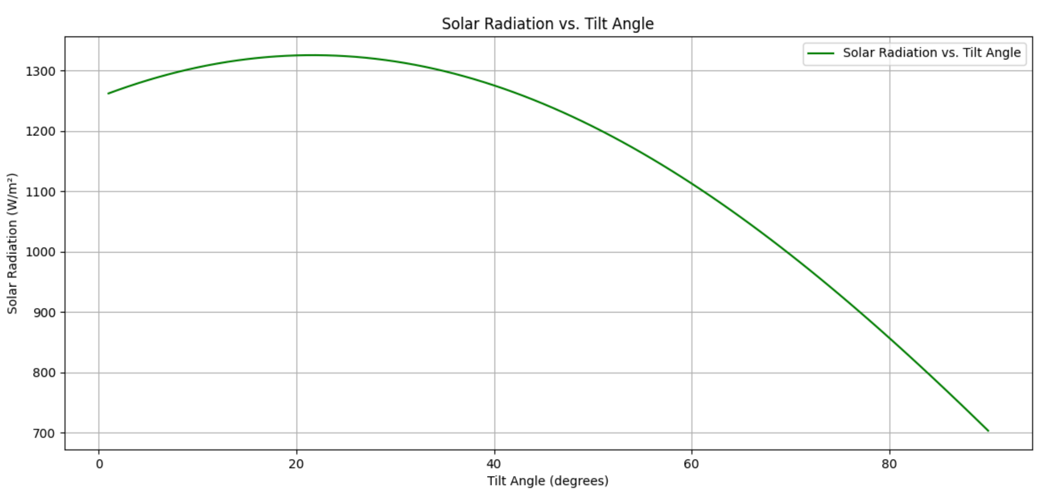

Figure 4.12: Variation of Optimum Tilt Angle for Raipur (Spring)

The percentage reduction in maximum solar radiation from Bangalore:

- Srinagar: 6.23% (84.12 W/m²)
- Raipur: 1.77% (24 W/m²)
- Bikaner: 3.8% (51.32 W/m²)
- Amritsar: 5.1% (69.62 W/m²)
- Guwahati: 3.1% (42.82 W/m²)

For Summer, we have taken the date to be June 21st. Guwahati leads with 1241.66 W/m² at 3°, while Bangaluru registers 1215.78 W/m² at 1°. Optimal tilt angles:

For Bikaner, as explained in Fig 4.13, the optimal tilt angle for maximum solar radiation during the spring season is 5°, with a total radiation of 1240.45 W/m². At the average tilt angle of 30°, the radiation decreases to 1154.75 W/m², highlighting the advantage of a 5° tilt for maximizing solar energy collection in this region.

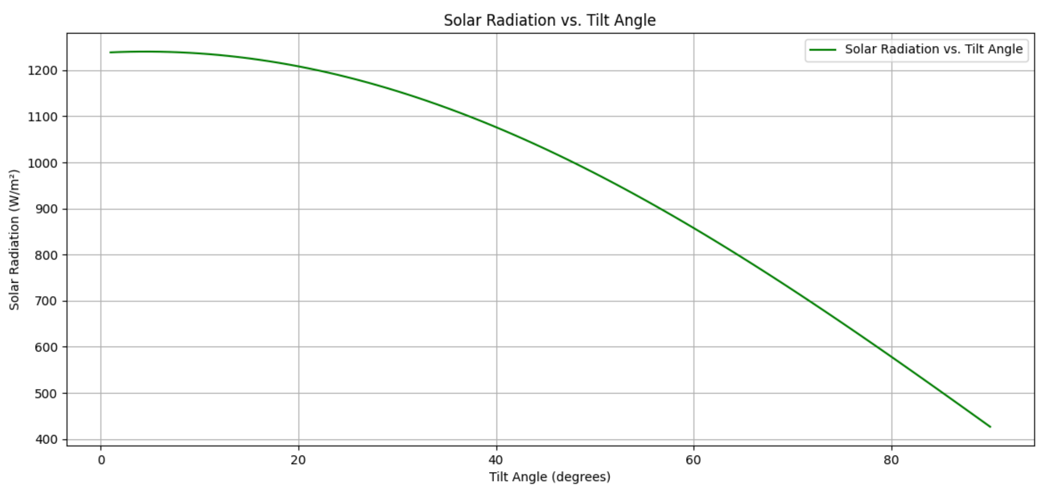

Figure 4.13: Variation of Optimum Tilt Angle for Bikaner (Summer)

For Amritsar, as explained in Fig 4.14, the optimal tilt angle for maximum solar radiation during the spring season is 8°, with a total radiation of 1236.94 W/m². At the average tilt angle of 30°, the radiation decreases to 1173.66 W/m², indicating that a 8° tilt provides better solar energy collection during this period. By adjusting the tilt to 8°, solar systems in Amritsar can achieve higher efficiency, leading to greater energy yield. The comparison highlights how fine-tuning tilt angles based on seasonal conditions can improve solar performance.

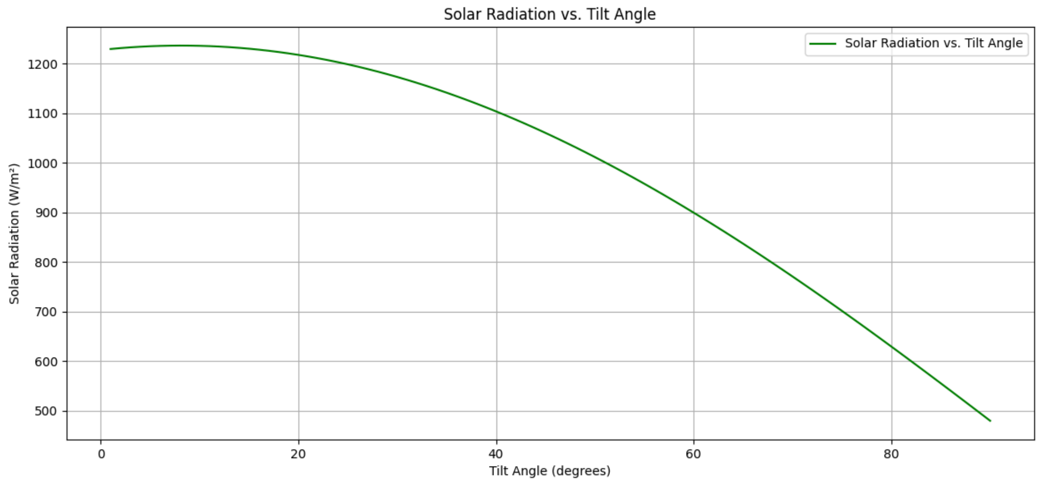

Figure 4.14: Variation of Optimum Tilt Angle for Amritsar (Summer)

For Srinagar, as explained in Fig 4.15, the optimal tilt angle for maximum solar radiation is 11°, with the total radiation reaching 1233.26 W/m². This is in contrast to the average tilt angle of 30°, which results in a solar radiation of 1183.30 W/m². This difference in radiation suggests that a tilt of 11° allows for a more efficient collection of solar energy.

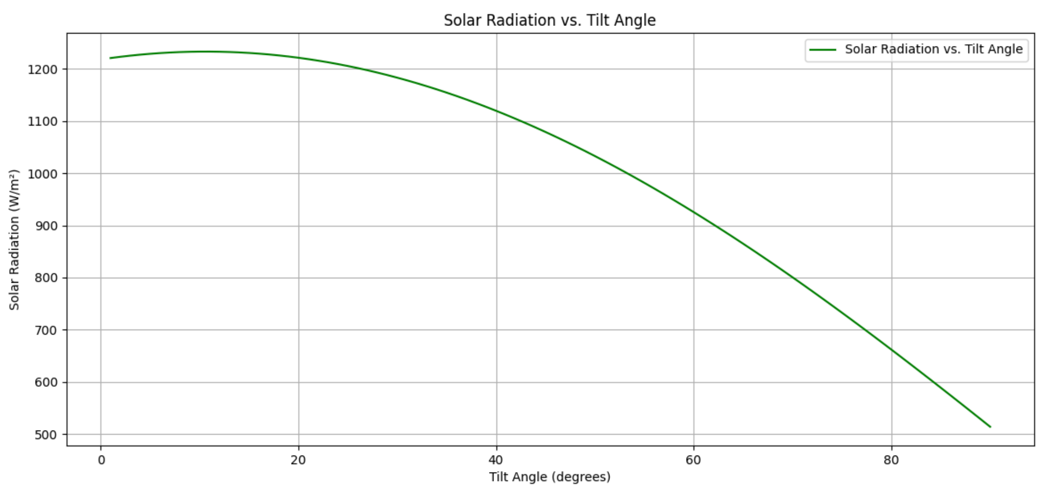

Figure 4.15: Variation of Optimum Tilt Angle for Srinagar (Summer)

For Bangalore, Refer Fig. 4.16, the optimal tilt angle for maximum solar radiation is 1°, with the total radiation reaching 1215.78 W/m². This is compared to the average tilt angle of 30°, which results in a solar radiation of 1022.17 W/m².

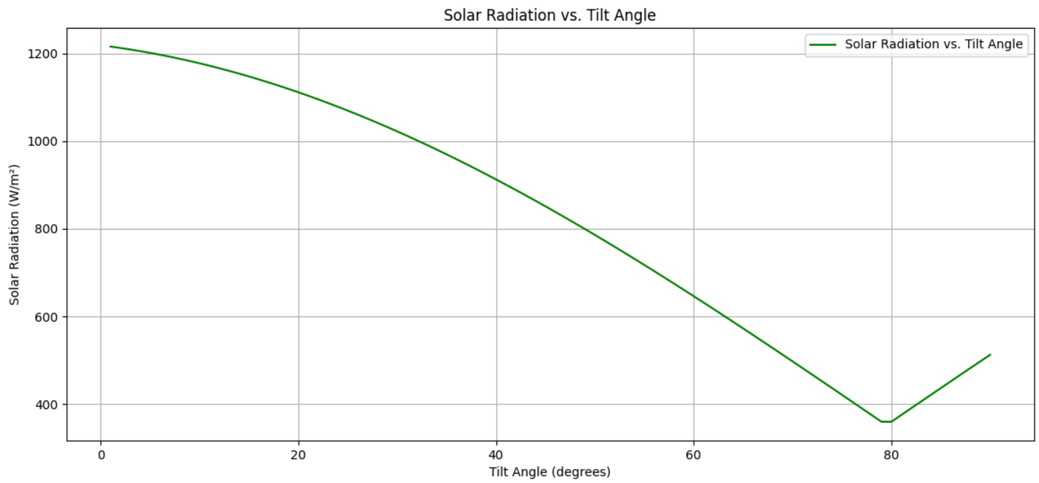

Figure 4.16: Variation of Optimum Tilt Angle for Bangalore (Summer)

For Guwahati, Refer Fig. 4.17, the optimal tilt angle for maximum solar radiation is 3°, with the total radiation reaching 1241.66 W/m². This is compared to the average tilt angle of 30°, which results in a solar radiation of 1142.97 W/m². The difference in radiation shows that adjusting the tilt angle can lead to a noticeable improvement in solar energy collection, even in regions with relatively high cloud cover or seasonal variations. By selecting the most efficient tilt angle, solar installations in Guwahati can achieve better energy performance and contribute to more effective utilization.

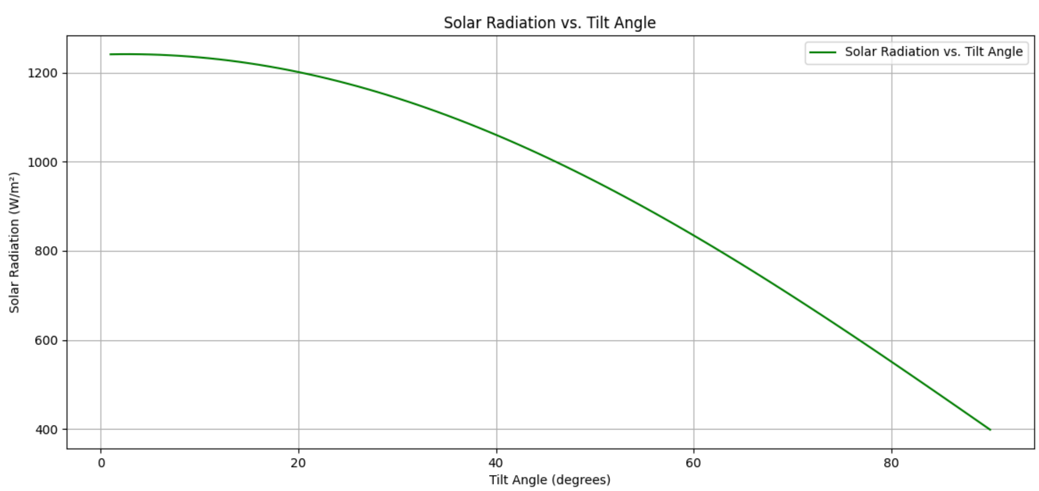

Figure 4.17: Variation of Optimum Tilt Angle for Guwahati (Summer)

For Raipur, Refer Fig. 4.18, the optimal tilt angle for maximum solar radiation is 1°, with the total radiation reaching 1240.45 W/m². In comparison, the average tilt angle of 30° results in a solar radiation of 1105.65 W/m².

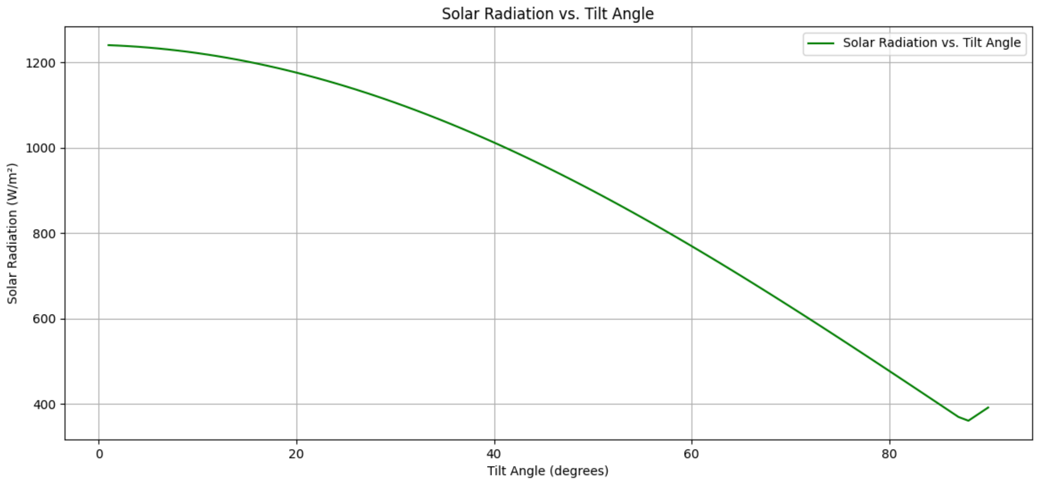

Figure 4.18: Variation of Optimum Tilt Angle for Raipur (Summer)

Reduction in solar radiation from Guwahati:

1) Srinagar: 0.67% (8.4 W/m²)
2) Raipur: 0.092% (1.2 W/m²)
3) Bikaner: 0.087% (1.09 W/m²)
4) Amritsar: 0.38% (4.72 W/m²)
5) Bangalore: 2.08% (25.92 W/m²)

Figures: Seasonal Variation of Tilt Angle at Six Different Cities

In Autumn, calculated on September 21st, Bangalore again leads with 1312.32 W/m² at 13°, while Srinagar registers 1229.40 W/m² at 34°. Optimal tilt angles:

For Bikaner, Refer Fig. 4.19, the optimal tilt angle for maximum solar radiation is 28°, with the total radiation reaching 1261.44 W/m². When using the average tilt angle of 30°, the solar radiation drops slightly to 1260.99 W/m². This small difference emphasizes that while the optimal tilt angle yields the highest solar energy collection, the average tilt angle still provides near-optimal performance. Adjusting tilt angles based on location-specific conditions ensures efficient solar energy harvesting, maximizing the energy production from solar panels in Bikaner. In autumn, as the sun's position in the sky changes, the optimal tilt angles for solar panels also shift to account for the lower solar altitude. In Bikaner, the tilt angle of 28° during this season ensures maximum solar radiation, which aligns with the lower sun angles typically observed during this time.The minimal difference in radiation between the optimal and average tilt angles demonstrates the ability to maintain high energy production even with slight variations in panel orientation, making autumn a suitable season for harnessing solar energy efficiently.

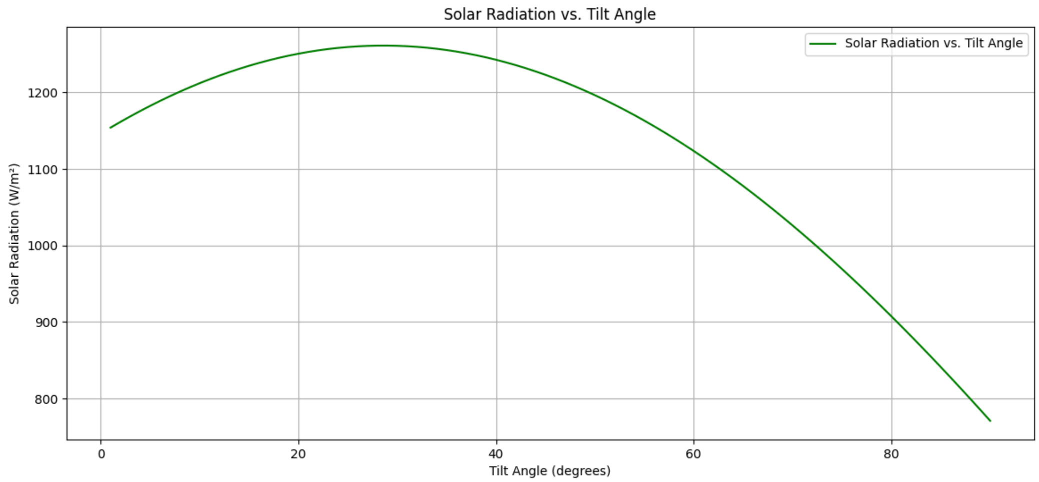

Figure 4.19: Variation of Optimum Tilt Angle for Bikaner (Autumn)

In Amritsar during autumn, Refer Fig. 4.20, the optimal tilt angle of 32° results in a total solar radiation of 1243.19 W/m², which is marginally higher than the radiation of 1242.71 W/m² achieved with the average tilt angle of 30°.

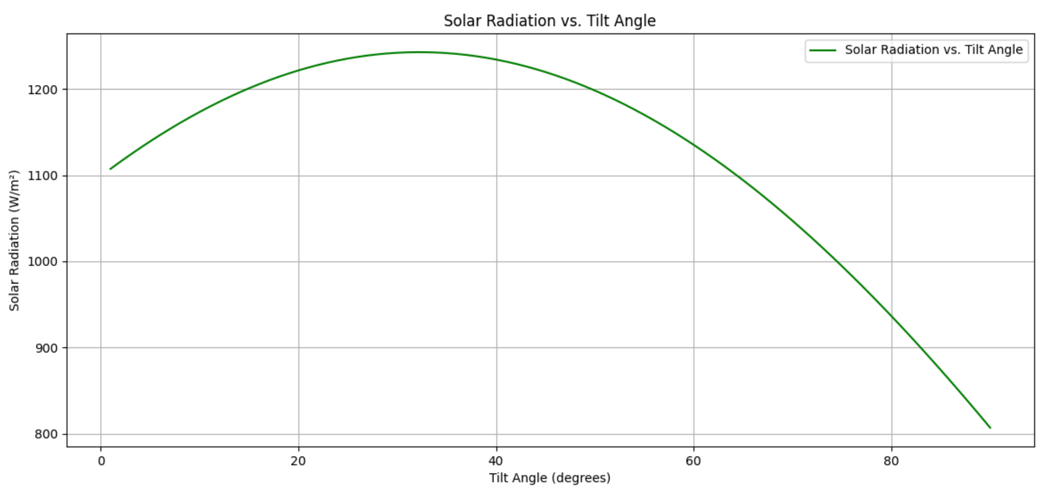

Figure 4.20: Variation of Optimum Tilt Angle for Amritsar (Autumn)

In Srinagar during autumn, as explained in Fig. 4.21, the optimal tilt angle of 34° results in a total solar radiation of 1229.41 W/m², slightly higher than the radiation of 1226.82 W/m² achieved with the average tilt angle of 30°. Although the difference is modest, it underscores the benefit of adjusting the tilt angle to the optimal position for maximizing solar energy capture. This ensures greater efficiency in solar systems, particularly in regions with variable seasonal solar radiation.

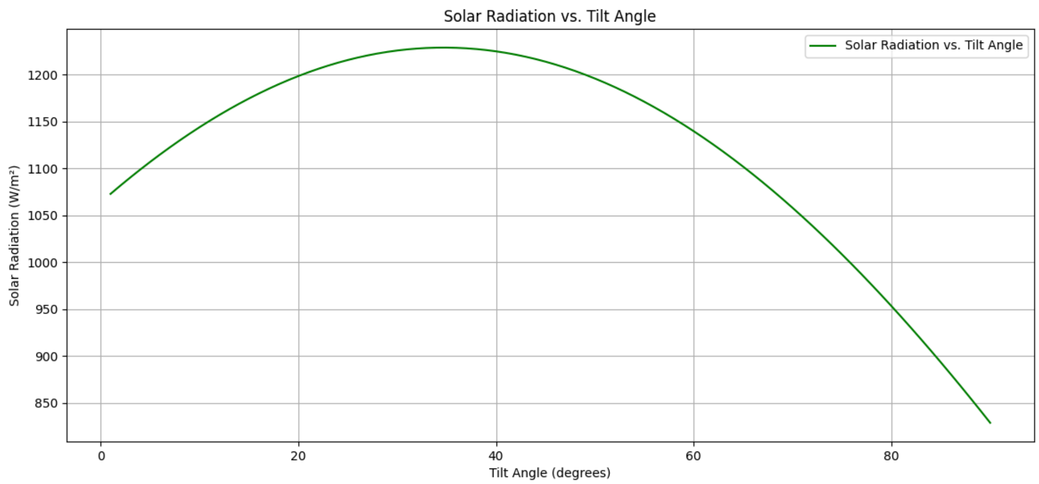

Figure 4.21: Variation of Optimum Tilt Angle for Srinagar (Autumn)

In Bangalore during autumn, as explained in Fig. 4.22, the optimal tilt angle of 13° results in a total solar radiation of 1312.32 W/m², compared to 1271.29 W/m² with the average tilt angle of 30°. This shows a noticeable increase in solar radiation by adjusting the tilt to 13°, highlighting the importance of considering local seasonal conditions.This small shift in angle can lead to better efficiency in harnessing solar energy in Bangalore's climate during autumn. For regions with similar weather patterns, applying this optimized tilt could enhance the performance of solar power systems, maximizing efficiency.

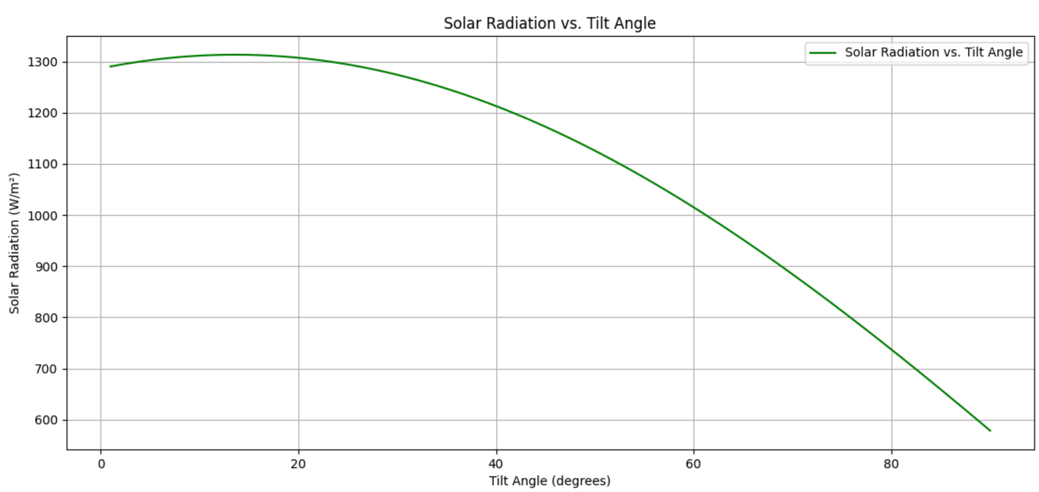

Figure 4.22: Variation of Optimum Tilt Angle for Bangalore (Autumn)

In Guwahati, as explained in Fig. 4.23, during autumn, the optimal tilt angle of 26° yields a solar radiation of 1269.89 W/m², while the average tilt angle of 30° results in 1267.98 W/m².

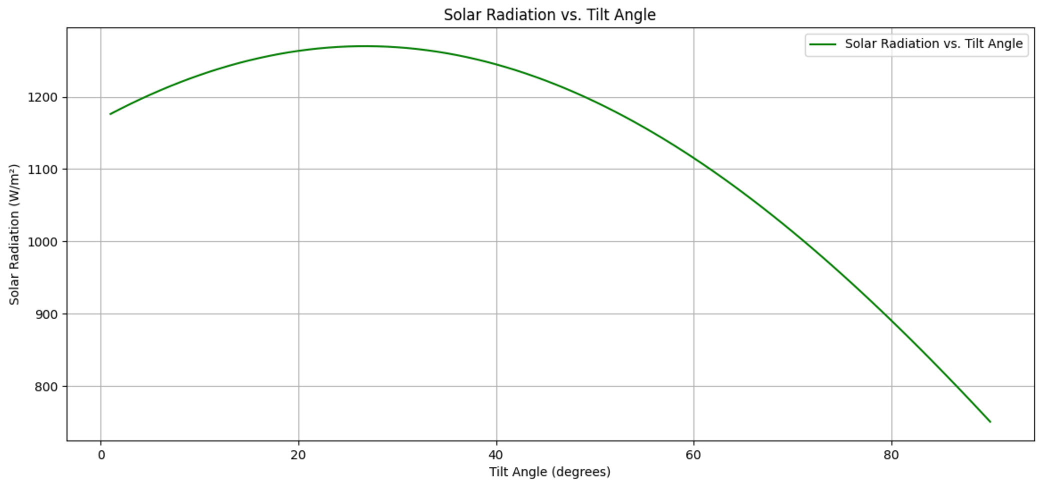

Figure 4.23: Variation of Optimum Tilt Angle for Guwahati (Autumn)

In Raipur, during autumn, as explained in Fig. 4.24 the optimal tilt angle of 21° results in a solar radiation of 1289.08 W/m², compared to the average tilt angle of 30° which gives 1278.55 W/m².

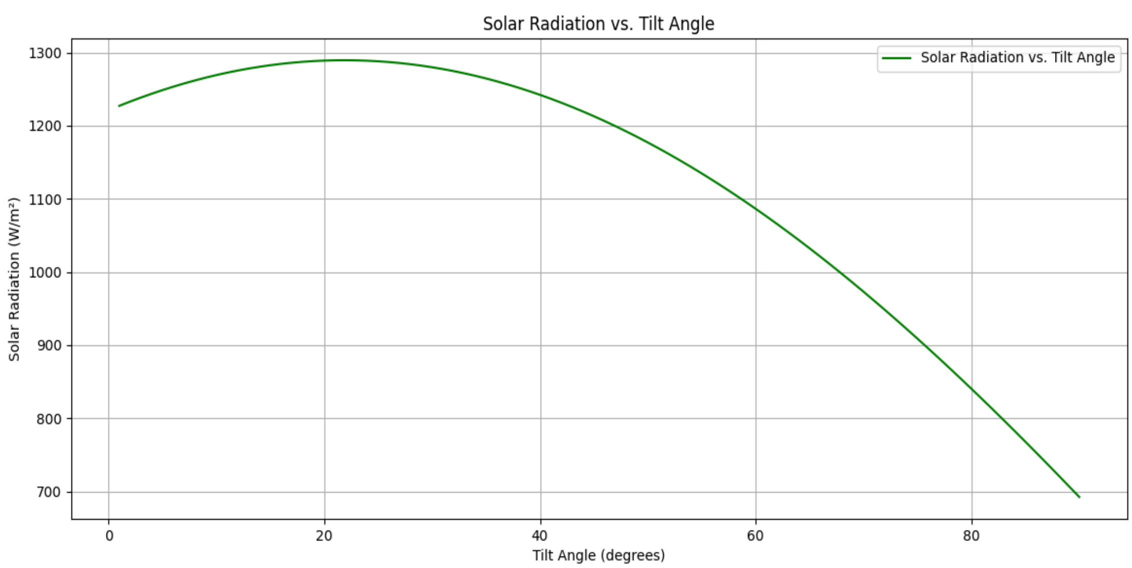

Figures 4.24: Variation of Optimum Tilt Angle for Raipur (Autumn)

Reduction in solar radiation from Bangalore:

- Srinagar: 6.31% (82.92 W/m²)
- Raipur: 1.77% (23.24 W/m²)
- Bikaner: 3.88% (50.88 W/m²)
- Amritsar: 5.26% (69.13 W/m²)
- Guwahati: 3.23% (42.44 W/m²)

The reduction in solar radiation across cities, as compared to Bangalore, highlights regional climatic and geographical differences. Srinagar exhibits the most significant drop, with a 6.31% decrease or 82.92 W/m², primarily due to its northern latitude and cooler climate. Conversely, Raipur shows minimal reduction at just 1.77% (23.24 W/m²), reflecting its favorable conditions for solar energy generation.

Bikaner's moderate decrease of 3.88% (50.88 W/m²) highlights the influence of its desert environment, where high solar irradiance is offset by seasonal variations. Amritsar's reduction of 5.26% (69.13 W/m²) is indicative of its temperate climate and occasional fog, particularly in winter. Meanwhile, Guwahati's 3.23% (42.44 W/m²) reduction emphasizes the impact of its subtropical climate, marked by high rainfall and humidity levels. These findings not only demonstrate the importance of regional tailoring in solar energy projects but also reinforce the need for advanced modeling techniques to account for local meteorological patterns when designing and optimizing solar installations.

This data underscores the need to optimize solar panel orientations and installations to maximize efficiency in different climatic zones.

Electricity Generation and Cost Analysis

This analysis highlights the comparison of electricity generation costs between the Average Tilt Angle (ATA) and the Optimal Tilt Angle (OTA) for each city, emphasizing the impact of tilt optimization on cost efficiency and energy production.

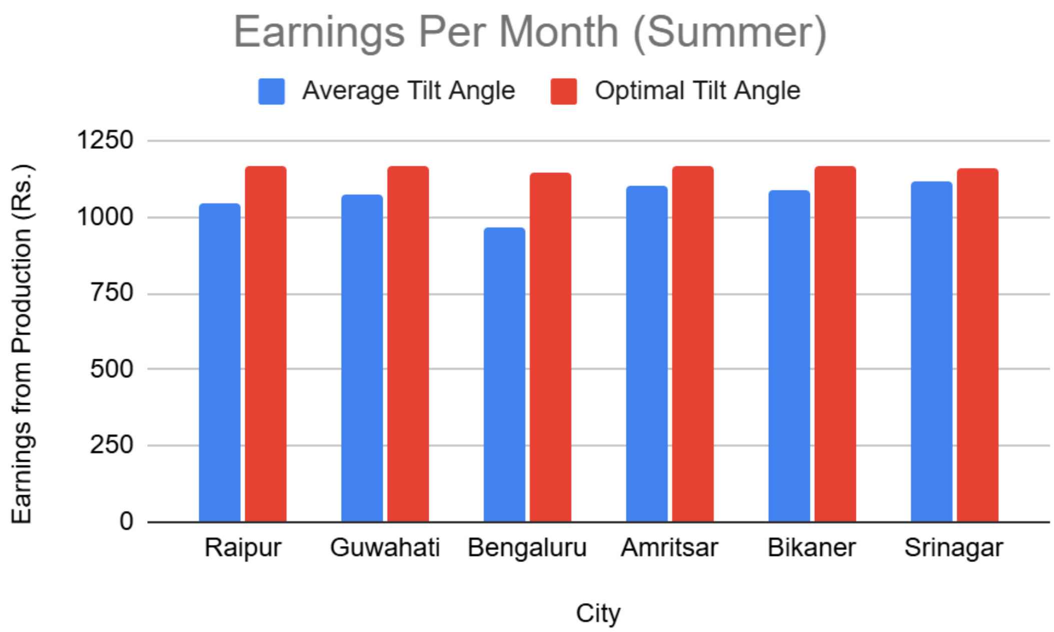

Figure 4.25: Earnings from Electricity Production (Summer)

For Summer, as explained in Fig. 4.25, leveraging the Optimal Tilt Angle (OTA) for solar panels results in noticeably higher earnings from electricity production compared to using the Average Tilt Angle (ATA). While the monthly difference per household may range between ₹100 and ₹150, this small margin becomes significant when accumulated across multiple households or an entire region. For individual homeowners, this increase translates to a more efficient return on investment for their solar energy systems. Over an extended period, the cumulative financial benefits grow substantially, contributing to greater savings and enhanced earnings for the community.

Moreover, the adoption of OTA aligns with sustainable energy goals by maximizing solar energy capture during peak sunlight months. This optimized energy production reduces reliance on conventional energy sources, further cutting down household energy costs and minimizing carbon footprints. Cities with higher adoption rates of OTA-based installations can also experience significant reductions in energy production costs and improved grid efficiency.

The economic implications extend beyond individual households, as increased efficiency contributes to a more resilient energy ecosystem. This highlights the importance of proper design, installation, and maintenance of solar systems to ensure the benefits of OTA are fully realized, supporting a greener and economically beneficial future for solar energy adopters.

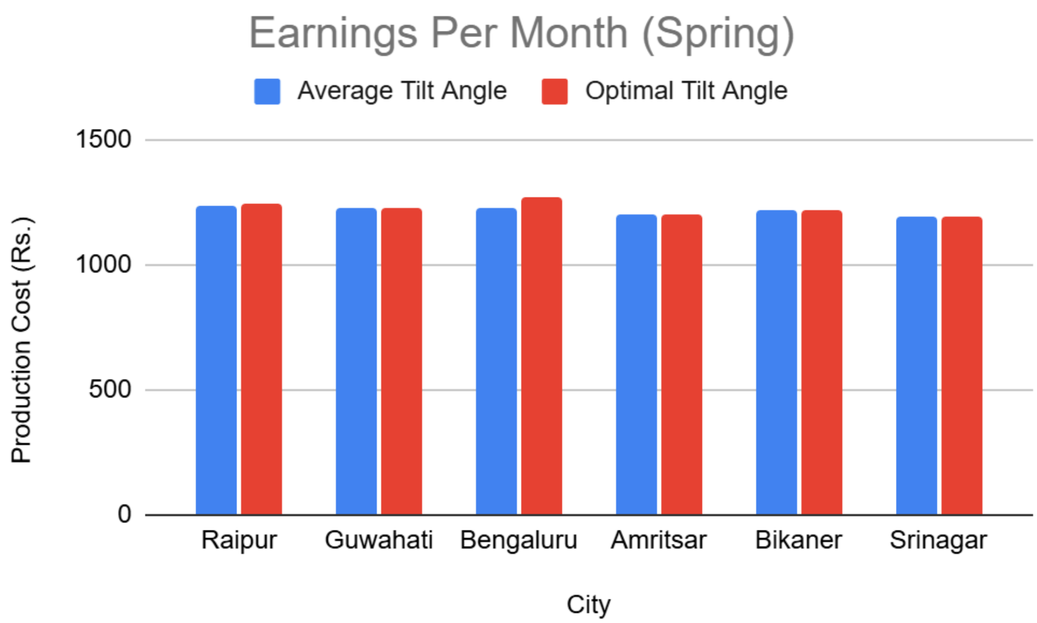

Figure 4.26: Earnings from Electricity Production (Spring)

The monetary difference between ATA and OTA earnings per household is negligible, reflecting the season's stable solar energy potential. Spring offers balanced sunlight conditions, reducing the impact of tilt adjustments on electricity generation.

As explained in Fig. 4.26, while the earnings remain close, cities with higher solar irradiation in spring may still benefit slightly from using the OTA, though the difference is less significant compared to other seasons. For example, cities like Srinagar and Bikaner, which experience more variation in other seasons, see less of a contrast in spring earnings due to the overall consistency in sunlight.

Overall, the spring season provides a steady performance for solar energy systems, offering homeowners reliability with minimal adjustments. However, optimizing for OTA is still beneficial for long-term energy production and cost savings across the year. It ensures the panels are positioned for peak efficiency year-round, which may translate into increased savings and energy production in the long run.

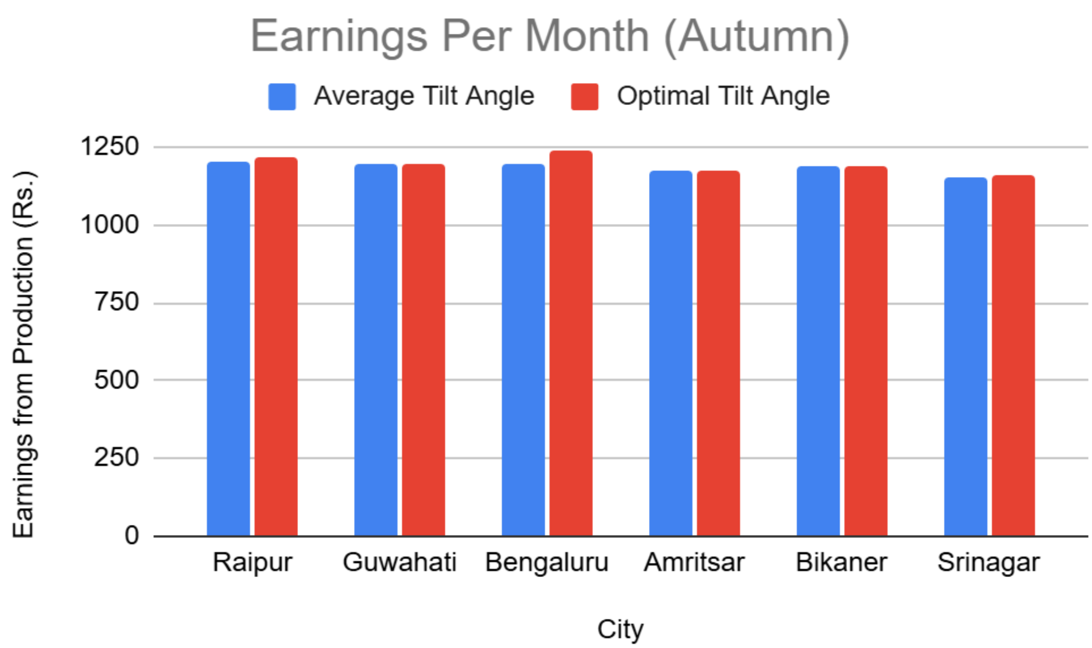

Figure 4.27: Earnings from Electricity Production (Autumn)

During autumn, as explained in Fig. 4.27, the impact of tilt angle optimization varies significantly across cities, with Bangalore showcasing the highest difference in electricity generation and earnings when comparing the Average Tilt Angle (ATA) to the Optimal Tilt Angle (OTA). This highlights the city's potential for maximizing energy production through precise adjustments. Bengaluru's geographical location and relatively high solar irradiance during autumn make it particularly sensitive to the choice of tilt angle, emphasizing the importance of system optimization for households to achieve better returns.

Conversely, cities like Amritsar and Srinagar exhibit the smallest difference between ATA and OTA values. This indicates a more consistent solar energy yield regardless of tilt adjustments, likely due to their higher latitude and reduced solar intensity in autumn. The minimal variation in these northern cities reflects a diminishing role of tilt optimization during this season, as the overall irradiation levels stabilize.

The disparity between cities underscores the role of geographic and climatic factors in solar energy generation. While tilt optimization yields noticeable benefits in regions like Bengaluru, its impact is less pronounced in Amritsar and Srinagar.

In Amritsar and Srinagar, the limited improvement reflects their higher latitude and cooler autumn conditions, where solar intensity is naturally lower. These regions might benefit more from advancements in solar panel efficiency or complementary energy strategies than from tilt optimization alone during autumn.

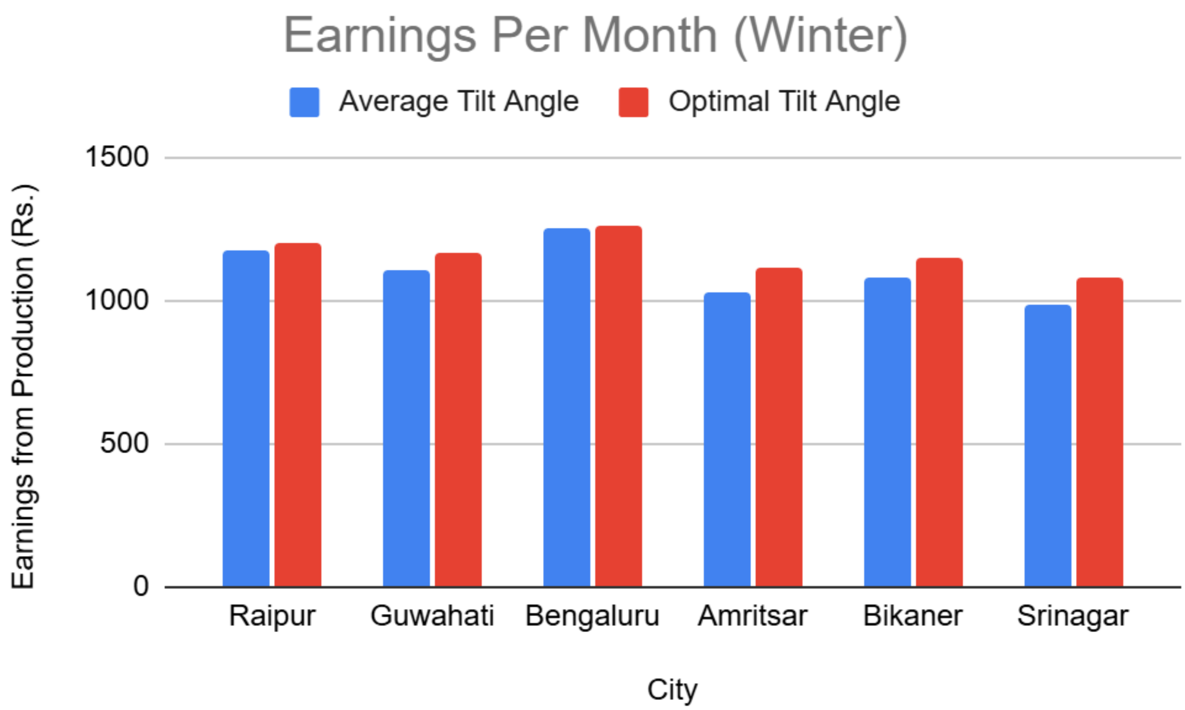

Figure 4.28: Earnings from Electricity Production (Winter)

During winter, as explained in Fig. 4.28, the earnings from solar energy generation across the six cities exhibit a considerable variation. Srinagar, located in the northernmost region, records the maximum difference in earnings due to its higher latitude, reduced solar intensity, and colder climate.

In contrast, Bengaluru, situated closer to the equator, experiences minimal seasonal variation in solar radiation.

The data presented in Table 4.1 highlights the roof area utilization for solar panel installations in High-Income Group (HIG) houses across the analyzed cities. By understanding the roof area utilization trends across different regions, policymakers make informed decisions regarding the adoption of solar technology. Cities with larger roof areas or more favorable conditions can accommodate higher numbers of panels, leading to increased energy production and cost savings.

Conversely, cities with limited roof space require optimal utilization strategies to balance energy needs with available space. This data also aids in assessing the scalability of solar installations, allowing for customized solutions that cater to specific energy demands while optimizing available resources. The analysis emphasizes the value of sustainable planning and design in urban residential settings, paving the way for wider adoption of renewable energy solutions in HIG houses.

Table 4.1: Roof area utilization for solar panel installations and the remaining area across the High-Income Group (HIG) houses in the analyzed cities.

City	HIG Roof Area (Sq.ft.)	% Installation	Installation Area	Area Consumed for Fulfilling Requirement		Area Remaining	
				In Sq. Ft.	In %	In Sq. Ft.	In %
Raipur	3700	20.00%	740.00	37	1	703.00	19
Guwahati	920	20.00%	184.00	32	3.47	152.00	16.52
Bengaluru	1000	20.00%	200.00	34.5	3.45	165.50	16.55
Amritsar	1250	20.00%	250.00	84.5	6.76	165.50	13.24
Bikaner	1200	20.00%	240.00	45	3.75	195.00	16.25
Srinagar	3600	20.00%	720.00	21	0.58	699.00	19.41

Electricity Generation and Cost Analysis

Detailed the comparison of electricity generation costs using solar panels vs. coal,

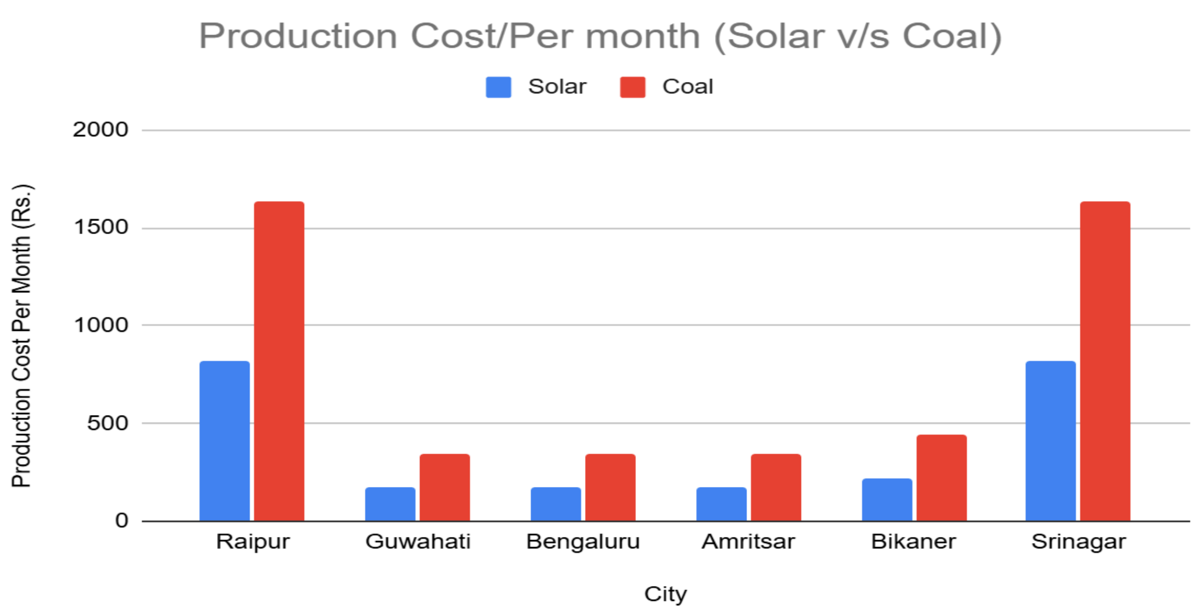

Figure 4.29: Cost Comparison of Electricity Generation for 1 household usage

The comparison of monthly electricity production costs, as explained in Fig. 4.29, between solar energy and coal across various cities highlights the economic advantage of adopting renewable energy solutions. Solar energy proves to be significantly cost-effective, offering substantial savings, particularly in regions with higher coal-dependent energy costs.

In Raipur, the monthly production cost for coal-powered energy is approximately ₹1600, whereas solar energy achieves the same production at just ₹800, reflecting a 50% reduction in cost. Guwahati further underscores the affordability of solar energy, with costs as low as ₹200 compared to ₹370 for coal. Bengaluru, despite its relatively higher solar energy production costs at ₹2200, still outpaces coal, which costs ₹380, demonstrating scalability in urban areas.

Amritsar and Bikaner, at ₹205 and ₹290 for solar energy respectively, offer similar cost reductions compared to coal, priced at ₹380 and ₹450. Meanwhile, Srinagar, despite its northern location and challenging conditions, benefits significantly from solar energy at ₹800 compared to the steep ₹1600 for coal.

These cost disparities emphasize the need for transitioning to solar energy to achieve long-term economic and environmental benefits. The data underscores solar energy's potential to offer affordable, sustainable energy solutions tailored to the unique needs of each city.

CO_2 Emissions Comparison

The stark contrast in CO_2 emissions between coal and solar energy highlights the environmental benefits of transitioning to renewable energy sources. Across all cities analyzed, solar energy consistently produces significantly lower CO_2 emissions per kilogram of energy generated, offering a sustainable alternative to coal-based energy production. Refer to Fig. 4.30.

In Raipur, coal energy emissions reach a staggering 295 kg of CO_2 per unit of energy, compared to just 20 kg from solar energy—a drastic reduction of over 93%. Similarly, Guwahati, Bengaluru, and Amritsar each emit 75 kg of CO_2 per unit with coal energy but achieve a mere 5 kg with solar energy, underscoring solar energy's uniform environmental efficiency in diverse climatic zones.

Bikaner exhibits a notable drop in emissions, from 88 kg for coal energy to just 4 kg for solar energy, highlighting its suitability for regions with high solar irradiance. Srinagar, despite its northern latitude, demonstrates substantial environmental gains by reducing emissions from 290 kg with coal to 14 kg with solar energy.

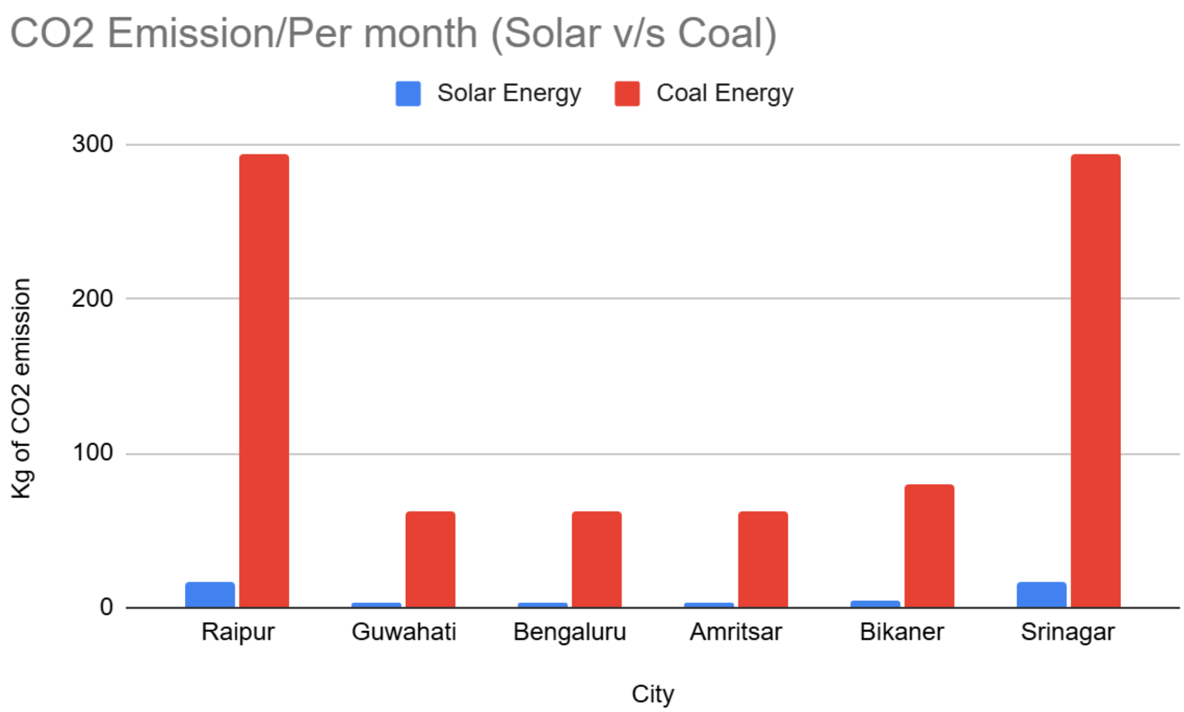

Figure 4.30: Comparison for CO2 Emissions per month for 1 household usage

As explained in Fig. 4.30, These findings emphasize the urgent need for widespread solar energy adoption. Beyond economic advantages, transitioning to solar energy is pivotal for reducing carbon footprints, combating climate change, and ensuring cleaner air for future generations. Solar energy is not just cost-effective but an imperative for a sustainable future.

Annual Tilt Angle Variation:

Figures 4.1 to 4.24 show the optimal tilt angles for different cities throughout the year. The ideal tilt angle ranges from:

- 1 - 45 degrees in Raipur
- 5 - 51 degrees in Bikaner
- 8 - 55 degrees in Amritsar
- 11 - 58 degrees in Srinagar
- 1 - 36 degrees in Bangalore
- 3 - 50 degrees in Guwahati

Seasonal Variation of Tilt Angles :

Seasonal fluctuations in solar irradiation were observed for six cities. For example, in Raipur, the maximum irradiation in winter is 1279.167 W/m², while in summer, it is 1240.45 W/m², with spring and autumn values of 1325.662 W/m² and 1289.08 W/m², respectively. This trend is similar for other cities, with varying levels of irradiation across different seasons.

Table of Optimum Tilt Angles :

Different tilt angles are required in each zone to achieve maximum solar irradiation throughout the year. These angles vary by season:

- Winter: 41.67° in Zone 1 (Raipur) to 33.33° in Zone 6 (Bangalore)
- Spring: 20° in Zone 1 to 13.33° in Zone 6
- Summer: 8.33° in Zone 1 to 6.67° in Zone 6
- Autumn: 21.67° in Zone 1 to 13.33° in Zone 6

Chapter – V

Conclusions

The study concluded the following optimal tilt angles for each zone throughout the year:

1. **Zone 1 (Raipur)**: 45° (winter), 22° (spring), 1° (summer), 21° (autumn)
2. **Zone 2 (Bikaner)**: 51° (winter), 28.33° (spring), 13.33° (summer), 28.33° (autumn)
3. **Zone 3 (Amritsar)**: 55° (winter), 31.67° (spring), 10° (summer), 31.67° (autumn)
4. **Zone 4 (Srinagar)**: 58° (winter), 34° (spring), 11° (summer), 34° (autumn)
5. **Zone 5 (Guwahati)**: 50° (winter), 25° (spring), 11.67° (summer), 26.67° (autumn)
6. **Zone 6 (Bangalore)**: 36° (winter), 13.33° (spring), 6.67° (summer), 13.33° (autumn)

By comparing average and optimal tilt angles (ATA and OTA), the study highlights significant improvements in solar irradiance, electricity generation, and cost-effectiveness, with efficiency gains reaching up to **12.19%** in regions like **Guwahati** during Summer. Cities such as **Bangalore** and **Raipur** showcased consistent high performance, while regions with greater seasonal variation, like **Srinagar** and **Amritsar**, benefited the most from tilt optimization. Economic analysis revealed substantial savings, with maximum yearly savings of **₹75,187.17** in Raipur during peak irradiance periods.

This research underscores the importance of location-specific optimizations for solar energy systems. By incorporating adaptive tilt mechanisms and data-driven insights, solar energy systems can significantly reduce carbon footprints, lower electricity costs, and enhance energy sustainability. The findings provide a roadmap for scalable solar energy solutions, emphasizing the need for geographically tailored policies to maximize India's solar potential across diverse climatic and regional conditions.

CODE

```
import math

def main():
    # Input variables
    l = float(input("Enter the latitude angles in degrees: "))
    N = float(input("Enter the day number: "))
    sa0 = input("Enter S for south, N for north, E for east and W for west facing: ")

    # Converting latitude to radians
    l1 = math.radians(l)

    # Determine the south angle
    if sa0 == 'S':
        sa = 0.0
    elif sa0 == 'N':
        sa = math.pi
    elif sa0 == 'E':
        sa = -math.pi / 2
    elif sa0 == 'W':
        sa = math.pi / 2

    # Initialize variables
    t = math.pi / 2
    ref = 0.6
    d = math.radians(360 * (284 + N) / 365)
    dd1 = 23.47 * math.sin(d)
    d1 = math.radians(dd1)
    fws1 = (1 + math.cos(t)) / 2
    fwg1 = ref * (1 - math.cos(t)) / 2
    fws = math.radians((1 + math.cos(t)) / 2)
    fwg = math.radians(ref * (1 - math.cos(t)) / 2)
    s2 = math.cos(math.radians(N * 360 / 365))
```

```
A = 1162.12 + (77.0323 * s2)
B = 0.171076 - (0.0348944 * s2)
C = 0.0897334 - (0.0412439 * s2)

arr = [45, 37.5, 30, 22.5, 15, 7.5, 0, -7.5, -15, -22.5, -30, -37.5, -45, -52.5, -60]
itarray = [0] * 15
itarray2 = [0] * 19
max_rad = 0

# Loop to calculate solar radiation for each angle in arr
for i in range(15):
    w = math.radians(arr[i])

    za2 = (math.cos(l1) * math.cos(w) * math.cos(d1)) + (math.sin(l1) * math.sin(d1))
    za1 = math.acos(za2)

    if za1 > math.pi / 2:
        za = za1 - (math.pi / 2)
    else:
        za = za1

    inc2 = (math.cos(l1) * math.cos(t) + math.sin(l1) * math.sin(t) * math.cos(sa)) * \
           (math.cos(d1) * math.cos(w)) + math.cos(d1) * math.sin(w) * math.sin(t) *
math.sin(sa) + \
           math.sin(d1) * (math.sin(l1) * math.cos(t) - math.cos(l1) * math.sin(t) *
math.cos(sa))
    inc1 = math.acos(inc2)

    if inc1 > math.pi / 2:
        inc = inc1 - math.pi
    else:
        inc = inc1

    rb = math.cos(inc) / math.cos(za)
```

```
        IDN = A * (math.exp((0 - B) / math.cos(za)))
        Id = C * IDN
        Ib = IDN * math.cos(za)
        It = Ib * rb + Id * fws1 + (Ib + Id) * fwg1

        itarray[i] = It
        max_rad = max(It, max_rad)
        print(f"Radiation for angle {arr[i]}: {It}")

    print(f"Maximum radiation = {max_rad}")

    # Find the angle corresponding to max radiation
    P = itarray.index(max_rad)
    w = math.radians(arr[P])

    TILTarr = [0, 5, 10, 15, 20, 25, 30, 35, 40, 45, 50, 55, 60, 65, 70, 75, 80, 85, 90]

    # Loop to calculate radiation for different tilt angles
    for j in range(19):
        t = math.radians(TILTarr[j])

        za2 = (math.cos(l1) * math.cos(w) * math.cos(d1)) + (math.sin(l1) * math.sin(d1))
        za1 = math.acos(za2)

        if za1 > math.pi / 2:
            za = za1 - (math.pi / 2)
        else:
            za = za1

        inc2 = (math.cos(l1) * math.cos(t) + math.sin(l1) * math.sin(t) * math.cos(sa)) * \
               (math.cos(d1) * math.cos(w)) + math.cos(d1) * math.sin(w) * math.sin(t) *
math.sin(sa) + \
               math.sin(d1) * (math.sin(l1) * math.cos(t) - math.cos(l1) * math.sin(t) *
math.cos(sa))
```

```
        inc1 = math.acos(inc2)

        if inc1 > math.pi / 2:
            inc = inc1 - math.pi
        else:
            inc = inc1

        rb = math.cos(inc) / math.cos(za)
        IDN = A * (math.exp((0 - B) / math.cos(za)))
        Id = C * IDN
        Ib = IDN * math.cos(za)
        It = Ib * rb + Id * fws1 + (Ib + Id) * fwg1

        itarray2[j] = It
        max_rad = max(It, max_rad)
        print(f"Radiation for {TILTarr[j]} degree tilt angle = {It}")

    print(f"Maximum radiation = {max_rad}")

    # Find the tilt angle corresponding to max radiation
    P = itarray2.index(max_rad)
    print(f"Maximum radiation of {max_rad} is at tilt angle = {TILTarr[P]}")

if __name__ == "__main__":
    main()
```

REFERENCES

A) **Journals / Articles**

1. Behar O, Khellaf A, Mohammedi K. A comparison of solar radiation models and their validation for the Algerian climate - focusing on direct irradiance. *Energy Convers Manag*. 2015 Jul 1;98:236–51.
2. Al-Sanea SA, Zedan MF, Al-Ajlan SA. Adjustments for the ASHRAE clear-sky model based on solar-radiation data in Riyadh. *Appl Energy*. 2004;79(2):215–37.
3. Jamil B, Khan MM, Maroof Khan M. Estimation of clear-sky solar radiation using the ASHRAE model for Aligarh, India. *International Journal of Engineering Research and Technology*. 2014;7. Available from: http://www.irphouse.com
4. Badescu V, Gueymard CA, Cheval S, Oprea C, Baciu M, Dumitrescu A, et al. Review and testing of 54 models for computing global and diffuse solar hourly irradiation on clear sky. *Renewable and Sustainable Energy Reviews*. 2012;16:1636–56.
5. Amarananwatana P, Sorapipatana C. Evaluation of the ASHRAE Clear Sky Model for irradiance prediction in Thailand. *Asian Journal on Energy and Environment*. 2007;2:523–32. Available from: www.asian-energy-journal.info
6. N&gomdov N. The improved ASHRAE model to predict hourly and daily solar radiation components in Botswana, Namibia, and Zimbabwe. *WREC 1996*.
7. B~aro S, Cannistraro G, Giaconia C, Orioli A. Evaluation of the ASHRAE clear sky model in the Mediterranean Zone. *Solar & Wind Technology*. 1988;5.
8. Gueymard C. Revising ASHRAE climatic data for design and standards - Part 2: Clear-sky solar radiation model. Available from: https://www.researchgate.net/publication/261179954
9. Khalid H, Zakaria M. Estimation of solar radiation in southern Pakistan using radiation models. *Journal of Renewable and Sustainable Energy*. 2016;8.
10. Ahmad MJ, Tiwari GN. A review of solar radiation models. *International Journal of Energy Research*. 2011;35:271–90.
11. El Mghouchi Y, Ajzoul T, El Bouardi A. Daily solar radiation intensity prediction by day of the year for 24 cities in Morocco. *Renewable and Sustainable Energy Reviews*. 2016;53:823–31.
12. Wong LT, Chow WK. Solar radiation model. Available from: www.elsevier.com/locate/apenergy
13. Western BE. The estimation of solar radiation in New Zealand. 1990;45.
14. Kontoleon KJ. Dynamic thermal circuit modelling with distribution of internal solar radiation on varying façade orientations. *Energy Build*. 2012 Apr;47:139–50.
15. Zhi-Gang R, Hu SG, Ding QJ. The effect of solar radiation model on temperature field of concrete-filled steel tube pier. 2010;27.

16. Yassin Alsadi S, Fathi Nassar Y, Alsadi S. Correction of the ASHRAE clear-sky model parameters based on solar radiation measurements in Arabic countries. *International Journal of Renewable Energy Technology Research*. 2016;5. Available from: http://ijretr.org1

B) **Conference Proceedings**

17. Abouhashish M. Applicability of ASHRAE clear-sky model based on solar radiation measurements in Saudi Arabia. In: *AIP Conference Proceedings*. 2017.

18. Maslensky V v., Bulygin YI, Temirkanov AR, Shchekina E v. Method selection for calculating heat supply from solar radiation to determine the climate system load of a mobile machine cabin. In: *IOP Conference Series: Materials Science and Engineering*. 2020.

C) **Books**

19. Tiwari GN. *Solar Energy Fundamentals, Design, Modelling and Applications*, Revised Edition, Narosa Publication House, New Delhi. 2002.

D) **Websites**

20. https://nptel.ac.in/courses/112105129

21. Centre for Policy Research (CPR): Trends in India's Residential Electricity Consumption (NITI Aayog India Energy). *Available at:* https://cprindia.org/trends-in-indias-residential-electricity-consumption/

22. Housing Board Project List. *Available at:* https://cghb.gov.in/project-list.html